

1 Solubility and Solution-phase Chemistry of Isocyanic Acid, Methyl Isocyanate,
2 and Cyanogen Halides
3
4

5
6 James M. Roberts¹, and Yong Liu²
7

8 *1. NOAA/ESRL Chemical Sciences Division, Boulder, Colorado, 80305*

9 *2. Department of Chemistry, University of Colorado, Denver, Denver, Colorado, 80217*
10
11
12
13
14
15
16
17
18
19
20
21
22
23
24
25
26
27
28
29
30
31
32
33
34
35
36
37
38
39
40
41
42
43
44
45
46
47
48
49
50
51

52 **Abstract**

53
54 Condensed phase uptake and reaction are important atmospheric removal processes for reduced nitrogen
55 species, isocyanic acid (HNCO), methyl isocyanate (CH₃NCO) and cyanogen halides (XCN, X = Cl, Br, I), yet many
56 of the fundamental quantities that govern this chemistry have not been measured or are understudied. These
57 nitrogen species are of emerging interest in the atmosphere as they have either biomass burning sources, i.e. HNCO
58 and CH₃NCO, or like the XCN species, have the potential to be a significant condensed-phase source of NCO⁻ and
59 therefore HNCO. Solubilities and first-order reaction rate of these species were measured for a variety of solutions
60 using a bubble flow reactor method with total reactive nitrogen (N_r) detection. The aqueous solubility of HNCO was
61 measured as a function of pH, and had an intrinsic Henry's law solubility of 20 (±2) M/atm, and a K_a of 2.0 (±0.3)
62 × 10⁻⁴ M (pK_a = 3.7 ± 0.1) at 298K. The temperature dependence of HNCO solubility was very similar to other small
63 nitrogen-containing compounds, such as HCN, acetonitrile (CH₃CN), and nitromethane, and the dependence on salt
64 concentration exhibited the "salting out" phenomenon. The rate constant of reaction of HNCO with 0.45 M NH₄, as
65 NH₄Cl, was measured at pH=3, and found to be 1.2 (±0.1) × 10⁻³ M⁻¹s⁻¹, faster than the rate that would be estimated
66 from rate measurements at much higher pHs. The solubilities of HNCO in the non-polar solvents n-octanol (n-
67 C₈H₁₇OH) and tridecane (C₁₃H₂₈) were found to be higher than aqueous solution for n-octanol (87 ± 9 M/atm at
68 298K) and much lower than aqueous solution for tridecane (1.7 ± 0.17 M/atm at 298K), features that have
69 implications for multi-phase and membrane transport of HNCO. The first-order loss rate of HNCO in n-octanol was
70 determined to be relatively slow 5.7 (±1.4) × 10⁻⁵s⁻¹. The aqueous solubility of CH₃NCO was found to be 1.3 (±0.13)
71 M/atm independent of pH, and CH₃NCO solubility in n-octanol was also determined at several temperatures and
72 ranged from 4.0 (±0.5) M/atm at 298K to 2.8 (±0.3) M/atm at 310K. The aqueous hydrolysis of CH₃NCO was
73 observed to be slightly acid-catalyzed, in agreement with literature values, and reactions with n-octanol ranged from
74 2.5 (±0.5) to 5.3 (±0.7) × 10⁻³ s⁻¹ from 298 to 310K. The aqueous solubilities of XCN ~~was~~ determined at room
75 temperature and neutral pH were found to increase with halogen atom polarizability from 1.4 (±0.2) M/atm for
76 ClCN, 8.2 (±0.8) M/atm for BrCN, to 270 (±54) M/atm for ICN. Hydrolysis rates, where measurable, were in
77 agreement with literature values. The atmospheric loss rates of HNCO, CH₃NCO, and XCN due to heterogeneous
78 processes are estimated from solubilities and reaction rates. Lifetimes of HNCO range from about 1 day against
79 deposition to neutral pH surfaces in the boundary layer, but otherwise can be as long as several months in the mid-
80 troposphere. The loss of CH₃NCO due to aqueous phase processes is estimated to be slower than, or comparable to,
81 the lifetime against OH reaction (3 months). The loss of XCNs due to aqueous uptake are estimated to range from
82 quite slow, lifetime of 2-6 months or more for ClCN, 1 week to 6 months for BrCN, to 1 to 10 days for ICN. These
83 characteristic times are shorter than photolysis lifetimes for ClCN, and BrCN, implying that heterogeneous
84 chemistry will be the controlling factor in their atmospheric removal. In contrast, the photolysis of ICN is estimated
85 to be faster than heterogeneous loss for average mid-latitude conditions.

86

87 I. Introduction

88
89 The earth's atmosphere is a highly oxidizing environment in which chemical compounds are typically
90 destroyed through radical pathways. The reduced nitrogen species, isocyanic acid (HNCO) and hydrogen cyanide
91 (HCN), are an exception to this, as they have slow reactions with atmospheric radicals and have primarily
92 condensed-phase sources and sinks (Li et al., 2000; Roberts et al., 2011). Cyanogen halides (XCN, where X = Cl,
93 Br, I) are compounds that are present in the environment, and whose atmospheric chemistry is of emerging interest.
94 XCN compounds likewise have very slow reaction rates with radical species and, with the exception of ICN, very
95 slow photolysis rates in the troposphere (Keller-Rudek et al., 2013). These general classes of reduced nitrogen
96 species, isocyanates (R-NCO), cyanides (RCN), and cyanogen halides (XCN) have potential health impacts that are
97 related to their condensed phase chemistry (Boenig and Chew, 1999; Broughton, 2005; McMaster et al., 2018;
98 Wang et al., 2007). Therefore, information on solubility and reaction rates are needed to understand the atmospheric
99 fate of such compounds and define their impact on human and ecosystem health. Five reduced nitrogen species will
100 be focused on here: isocyanic acid, HNCO, methyl isocyanate, CH₃NCO, which are biomass burning products, and
101 cyanogen chloride, ClCN, cyanogen bromide, BrCN, and cyanogen iodide, ICN, which could be condensed-phase
102 sources of cyanate ion (NCO⁻) and therefore HNCO.

103 The isocyanate compounds are products of the pyrolysis or combustion of N-containing materials (biomass,
104 polyurethanes) (Blomqvist et al., 2003; Koss et al., 2018) and the two simplest ones, HNCO and CH₃NCO, have
105 also been observed in interstellar and cometary media (Goesmann et al., 2015; Halfen et al., 2015). The atmospheric
106 chemistry of HNCO has received considerable attention in the past few years as it has become clear that it is present
107 in ambient air, and could be related to health impacts through specific biochemical pathways (Roberts et al., 2011)
108 involving the reaction of cyanate ion with proteins. There are relatively few observations of HNCO in ambient air,
109 showing "background" mixing ratios that range from 10pptv to over several ppbv depending on the nature of
110 regional sources, and peak mixing ratios approaching a few ppbv, observed in areas impacted by local biomass
111 burning (Chandra and Sinha, 2016; Kumar et al., 2018; Mattila et al., 2018; Roberts et al., 2014; Sarkar et al., 2016;
112 Wentzell et al., 2013; Woodward-Massey et al., 2014; Zhao et al., 2014). The aqueous phase solubility of HNCO
113 was examined by Roberts et al., (Roberts et al., 2011) and Borduas et al., (2016), wherein it was found that HNCO
114 shows behavior typical of weak acids, where the effective Henry's coefficient H_{eff} varies with pH, and so HNCO is
115 only slightly soluble at pHs characteristic of atmospheric aerosol (pH= 2-4) and is quite soluble at physiologic
116 conditions (pH=7.4). Attempts to model the global distribution of HNCO (Young et al., 2012) and the cloud water
117 uptake of HNCO (Barth et al., 2013) used the limited solubility and hydrolysis data available at that time, (Jensen,
118 1958; Roberts et al., 2011). Several aspects of HNCO solubility remain unknown, such as salt effects on aqueous
119 solubility, and solubility in non-aqueous solvents, a property important for predicting HNCO behavior in biological
120 systems. The pH dependent hydrolysis of HNCO had been studied some time ago (Jensen, 1958), the mechanism
121 for this process involves three separate reactions;

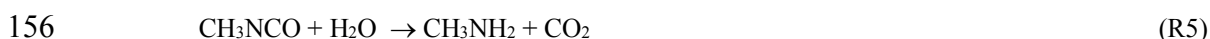
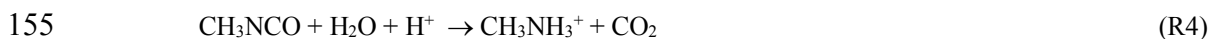




125 and Borduas et al. (2016), recently re-measured these rates under a wider range of conditions and found their
126 measurements to be essentially consistent with the previous work at pHs of interest in the atmosphere. Rates of
127 reaction of HNCO with other compounds in aqueous solution are not as well studied, especially under atmospheric
128 conditions, e.g. low pH, relatively high ionic strength. Rates of reaction of HNCO/NCO⁻ with nitrogen bases have
129 been measured but only at the pK_{as} of the BH⁺, which are typically pH 9-10 (Jensen, 1959; Williams and Jencks,
130 1974a, b). The pK_a is defined as the negative Log₁₀ of the dissociation constant of an acid, and can be thought of as
131 the pH at which the acid and its conjugate base (in this case BH⁺ and B) are at the same concentration.

132 Methyl isocyanate is most notable for its part in the one of the largest industrial disasters in history, when a
133 large quantity of CH₃NCO was released from a chemical plant and fumigated the city of Bhopal, India. There are
134 other, more common sources of CH₃NCO to the atmosphere including combustion of biomass (Koss et al., 2018)
135 and N-containing polymers such as polyurethanes and isocyanate foams (Bengtstrom et al., 2016; Garrido et al.,
136 2017), and cooking (Reyes-Villegas et al., 2018). Recent measurements of CH₃NCO in laboratory wildfire studies
137 have observed mixing ratios up to 10 ppbv or so in fuels characteristic of western North America (Koss et al., 2018).
138 CH₃NCO is also produced in photochemical reactions of methylisothiocyanate (CH₃NCS), which is the main
139 degradation product of the agricultural fungicide metam-sodium (CH₃NHCS₂Na) (Geddes et al., 1995). In addition,
140 CH₃NCO has been observed in studies of the photooxidation of amides (Barnes et al., 2010; Borduas et al., 2015;
141 Bunkan et al., 2015) and by extension will be formed in dimethyl amine oxidation. To our knowledge there is only
142 one reported set of ambient measurements of CH₃NCO, conducted near a field where metam-sodium was being used
143 as a soil fumigant (Woodrow et al., 2014), and the resulting CH₃NCO mixing ratios were as high as 1.7 ppbv. The
144 California Office of Environmental Health Hazard Assessment has placed an inhalation reference exposure level of
145 0.5 ppbv (1 µg/m³) on CH₃NCO due to its propensity to cause respiratory health effects (California, 2008).

146 There have been only a few studies of the gas phase loss rates of CH₃NCO including reaction with OH
147 radical, which appears to be slow based on the mostly recent measurements (Lu et al., 2014) (Papanastasiou et al., in
148 preparation, 2019), reaction with chlorine atoms (Cl) which might be as much as 20% of OH under some
149 atmospheric conditions (Papanastasiou et al., in preparation, 2019), and UV photolysis which has a negligible
150 contribution to atmospheric loss (Papanastasiou et al., in preparation, 2019). Thus, heterogeneous uptake might
151 compete with these gas phase loss processes. The solubility of CH₃NCO has not been previously determined
152 experimentally, but is probably low, <2 M/atm, by analogy to CH₃NCS (3.7 M/atm) (Geddes et al., 1995). In
153 addition, there are no data on the solubility of CH₃NCO in non-aqueous solvents. The hydrolysis of CH₃NCO is acid
154 catalyzed, exhibiting the following overall reactions;



157 producing methyl amine and carbon dioxide. The rate constants for these reactions are fairly well established (Al-
158 Rawi and Williams, 1977; Castro et al., 1985).

159 Cyanogen halides are less well studied as atmospheric species, but have potentially important
160 environmental sources. Cyanogen chloride was once produced as a chemical warfare agent, however its importance

161 to the atmosphere is more related to its possible formation in the reaction of active chlorine species (HOCl/OCl-,
162 chloramines) with N-containing substrates such as amino acids and humic substances (Na and Olson, 2006; Shang et
163 al., 2000; Yang and Shang, 2004). These reactions are known to be important in systems where chlorination is used
164 for disinfection such as swimming pools and water treatment (see for example (Afifi and Blatchley III, 2015), and
165 perhaps indoor surfaces (J. Abbatt, personal communication). We are not aware of any measurements of ClCN in
166 ambient air. Cyanogen bromide can likewise be formed through reactions of HOBr/OBr- with reduced nitrogen
167 species, and there are observations of BrCN in bromide-containing waters that have been received chlorine
168 treatment (see for example (Heller-Grossman et al., 1999). The formation results from the facile reaction of
169 HOCl/OCl- with bromide to make HOBr/OBr-, which then reacts with nitrogen species in the water. In addition,
170 there is a natural source of BrCN from at least one strain of marine algae (Vanellander et al., 2012) that is thought
171 to be related to allelopathic activity, i.e. secreted to control the growth of competing organisms. This marine algae
172 source may be responsible for BrCN levels observed in remote atmospheres (J.A. Neuman and P.R. Veres, personal
173 communication),(NASA, 2019). Cyanogen iodide can also potentially be formed from the chlorination of water or
174 wastewater because iodide is easily oxidized by HOCl/OCl-, however iodide is usually quite small in concentration,
175 so the several studies that report total cyanogen halides report ClCN and BrCN but not ICN (Diehl et al., 2000;
176 Yang and Shang, 2004). There are also biochemical pathways for ICN formation involving several enzymes that are
177 part of the immune defense system (see for example (Schlorke et al., 2016)), but the extent to which ICN might be
178 volatilized from those systems is not clear. There are also some observations of ICN in the remote marine
179 troposphere (J.A. Neuman and P.R. Veres, personal communication), but their origin is currently unclear.

180 The possible gas phase loss processes of cyanogen halides include reaction with radicals or ozone, and
181 photolysis. Radical reaction rates (OH, Cl) have not been measured at room temperatures, but are likely to be slow
182 due to the strength of X-CN bonds (Davis and Okabe, 1968). The UV-visible absorption spectra of all three of these
183 compounds have been measured (Barts and Halpern, 1989; Felps et al., 1991; Hess and Leone, 1987; Russell et al.,
184 1987), and indicate a range of photolysis behavior ranging from no tropospheric photolysis of ClCN, to slight
185 photolysis of BrCN, and faster photolysis of ICN. The rates of photolysis need to be balanced against condensed
186 phase losses of XCN compounds to obtain a full picture of their atmospheric losses.

187 The aqueous phase solution chemistry of cyanogen halides is not as well studied as the isocyanates. The
188 aqueous solubilities of XCN compounds are not known with the exception of ClCN whose solubility is thought to be
189 fairly low, 0.6 – 0.52 M/atm at 293-298K (Weng et al., 2011; Yaws and Yang, 1992) as reported by (Hilal et al.,
190 2008). The hydrolysis of XCN compounds are known to be base-catalyzed and so involve the following reactions;

191



194

195 with R6 being fairly slow at medium to low pH (Bailey and Bishop, 1973; Gerritsen et al., 1993). The product,
196 cyanic acid, HOCN, is unstable with respect to HNCO in aqueous solution (Belson and Strachan, 1982);

197



199
200 Thus, XCN compounds represent potential intermediates in the condensed-phase formation of HNCO, for which
201 there is some observational evidence (Zhao et al., 2014). So, in addition to being active halogen species, XCN
202 compounds represent potential condensed phase source of HNCO in systems where there is halogen activation and
203 there are reduced nitrogen species present, e.g. wildfire plumes, bio-aerosols and indoor surfaces.

204 Measurements of solubility and reaction rates will be presented here for HNCO, CH₃NCO, and the XCN
205 species: ClCN, BrCN, and ICN. The aqueous solubility of HNCO was measured as a function of pH in the range pH
206 2-4, temperature in the range 279-310K, and salt concentration up to 2.5M NaCl. The rate of reaction of HNCO with
207 NH₄⁺ was measured at pH3, to examine the importance of this reaction to atmospheric uptake of HNCO. The
208 solubilities of HNCO in the non-polar solvents n-octanol and tridecane were also measured as a function of
209 temperature, in the range 298-310K, and the first-order loss rate of HNCO in n-octanol was also determined. The
210 aqueous solubility of CH₃NCO was measured ~~at several~~ at several pHs pH 2 and 7, and the solubility in n-octanol
211 was also determined at several temperatures, 298 and 310K. Finally, the aqueous solubility of ClCN, BrCN, and
212 ICN were determined at room temperature, and at 273.15 K (ClCN, BrCN) and neutral pH, and the solubility and
213 first loss of these compounds in n-octanol was also determined. These data will be used to estimate atmospheric
214 lifetimes against aqueous uptake and to assess the relative bioavailability of these compounds.

215
216 **II. Methods**

217 Most of the techniques used for the work presented here have largely been presented elsewhere (Borduas et
218 al., 2016; Kames and Schurath, 1995; Kish et al., 2013; Roberts, 2005) and will only be briefly summarized here.
219 The basic principle is that the compound of interest is equilibrated with solution in a bubble flow reactor, and then
220 removed from the gas-phase and the exponential decay of the signal due to loss of the compound is measured with a
221 sensitive and selective method. The dependence of decay rates on flow rate-to-liquid volume ratio can then be
222 related to solubility and first-order loss rate due to reaction in solution. This technique relies on being able to
223 produce a consistent gas stream of the compound of interest, and being able to selectively detect the compound
224 exiting the reactor. This method has limitations in that the solubility must be within a certain range, and the first-
225 order loss rate slow enough that there are measurable amounts of compound exiting the reactor.

226
227 **A. Preparation of Gas-Phase Standards**

228
229 The general system used for preparation of gas phase streams of HNCO, CH₃NCO, BrCN, and ICN was the
230 capillary diffusion system described by (Williams et al., 2000) and (Roberts et al., 2010). Isocyanic acid was
231 produced in a steady stream by heating the trimer, cyanuric acid (Sigma-Aldrich, USA) to 250°C under N₂ and
232 establishing a constant diffusion rate through a short length of capillary tubing (1mm ID x 5cm length). Care was
233 taken to condition the system for several days before use, by keeping the system under flow and at a minimum of

234 125°C even when not in active use, to prevent the build-up of unwanted impurities, particularly NH₃. Standards in
235 the range of several ppmv in 40 SCCM could easily be prepared in this way.

236 The same capillary diffusion cells were used for CH₃NCO preparation, starting with a sample of the pure
237 liquid (Alinda Chemicals, UK). FTIR analysis of samples of this material were found to contain small amounts of
238 siloxanes (3% by mole), which probably came from a chloro-silane added as a stabilizer, but no measurable
239 presence of any other nitrogen compounds. The high volatility of CH₃NCO (BP 38 °C) required that low
240 concentration solution (1% vol/vol) of CH₃NCO in n-tridecane (C₁₃H₂₈) solvent at a temperature of 0°C be used in
241 the diffusion cell. Under these conditions a 40 SCCM stream resulted in a mixing ratio of 10ppmv. The output of the
242 source was stable for long periods of time (days) and could be used for the solubility study and calibration of other
243 instruments. The source was also analyzed by an H₃O⁺ chemical ionization mass spectrometric system (H₃O⁺ CIMS)
244 (Koss et al., 2018; Yuan et al., 2016), which showed that it had no impurities detectable above the 1% (as N) level.

245 The preparation of a gas phase standard of ClCN is described by Stockwell et al., (2018) and is based on
246 chemical conversion of an HCN calibration mixture. It has been known for some time that HCN reacts readily with
247 active chlorine compounds to yield ClCN (Epstein, 1947), for example:



249 In fact, this reaction has been used as the basis for measuring HCN in the gas phase by conversion to ClCN with
250 detection by gas chromatography with electron capture (Valentour et al., 1974). In those systems, Chloramine-T (*N*-
251 Chloro-*p*-toluenesulfonamide sodium salt, Sigma-Aldrich) has proven useful. The method used in this work
252 consisted of passing a small stream (5-10 SCCM) of a commercially-prepared 10ppmv gas-phase standard of HCN
253 in N₂ (GASCO, Oldsmar, FL), combined with humidified Zero Air (ZA, 80% RH, 30-50 SCCM) over a bed packed
254 with glass beads coated with a solution of Chloramine-T. The glass beads were prepared by coating glass 3 mm OD
255 beads with a 2 g/100cc solution and packing ~20cc of them in a 12.7mm OD PFA tube and flowing ZA over them
256 until they appeared dry. The reaction was shown to be essentially 100% (±10%) when conducted in a humidified
257 atmosphere (RH ≥60%), (H₃O⁺ CIMS), and FTIR analysis of the gas stream before and after passing through the
258 chlorination bed. The ClCN source was also checked by measuring the total nitrogen content of the gas stream
259 before and after the chlorination step, and the resulting signal was found to be 98±1% of the original HCN standard.
260 This means that the combination of the chlorination reaction and N_r conversion (see below) were at least 98%
261 efficient.

262 Preparation of BrCN and ICN gas streams was accomplished with the diffusion cell apparatus using
263 commercially available samples of BrCN (98% purity, Sigma-Aldrich) and ICN (97% purity ACROS Organics),
264 that were used without further purification. BrCN is a volatile solid, so was kept on a diffusion cell at 0°C while in
265 use. ICN is a relatively non-volatile solid and so was placed in a diffusion cell and heated to 80°C while in use.
266 These resulted in sample streams that were on the order of 250-350 ppbv in 1 SLPM in mixing ratio. Analysis by
267 iodide ion chemical ionization mass spectrometry {Warneke, 2016 #1366} indicated traces of the molecular halogen
268 species (Br₂, I₂), but no other significant N-containing species.

269
270

271 B. Detection of Nitrogen Compounds

272

273 The method for detection of the compounds studied in this work relies on high temperature conversion of
274 any N-containing species, except for N₂ or N₂O, to nitric oxide (NO) and detection of the resulting NO by O₃
275 chemiluminescence (Williams et al., 1998). This technique, which we will refer to as Total Reactive Nitrogen, N_r,
276 has been shown to measure a wide range of reduced nitrogen species as well as the more familiar oxides of nitrogen
277 (Hardy and Knarr, 1982; Saylor et al., 2010; Stockwell et al., 2018), provided care is taken to convert any nitrogen
278 dioxide that is formed in the Pt converter back to NO prior to detection (Schwab et al., 2007). In this work, this was
279 accomplished with a solid molybdenum tube operated at between 350 and 450 °C, with the addition of a small
280 amount of pure H₂ resulting in a 0.8% mixing ratio in the catalyst flow. The detection system was routinely
281 calibrated with a NO standard (Scott-Marrin, Riverside, CA) and the conversion efficiency was confirmed with a
282 low concentration (10ppmv) HCN standard (GASCO, Oldsmar, FL). The high conversion efficiencies (≥98%) for
283 HNCO and ClCN were confirmed by other methods as described by Stockwell et al. (2018). The conversion
284 efficiencies for BrCN, and ICN are assumed to be equally high due to the fact the X-CN bond strengths of these
285 compounds are lower than for H-CN and Cl-CN (Davis and Okabe, 1968) and the CH₃-NCO bond is weaker than
286 the H-NCO bond (Woo and Liu, 1935) so CH₃NCO should be easily converted by the N_r catalyst. Although readily
287 measured here, a solubility measurement of this kind does not require the determination of the absolute
288 concentration of the analytes, it only requires that the measurement be linear (i.e. constant sensitivity) throughout the
289 range of signals measured. The NO instrument is linear from the low pptv into the low ppmv range, the chief
290 limitation being the ability to count photon rates above 5MHz. The magnitude of the gas phase sources used and the
291 flow rate of the instrument (1 SLPM) insured that instrument signals did not reach the non-linear range.

292 The requirement for the detection method to be selective could be an issue with a general method such as
293 N_r. In practice, the reactions of the nitrogen species studied here form products that are not volatile under the
294 conditions used in this work, and so do not interfere with the measurement. In aqueous-phase reactions, HNCO
295 produces NH₃/NH₄⁺, CH₃NCO produces CH₃NH₂/CH₃NH₃⁺, and XCN compounds produce HOCN/NCO⁻ all of
296 which are non-volatile in the pH ranges at which those experiments were conducted. The products of the organic-
297 phase reactions are not as well known: tridecane should not react with HNCO, n-octanol will form carbamyl or
298 methyl carbamyl groups with n-octyl substituents which should be non-volatile. Possible reactions of XCN
299 compounds with n-octanol are less well known, particularly in the absence of water in the solution, so those
300 experiments will need to be interpreted with care.

301 The reactor used for the most of the experiments is a modification of the one described by Roberts (2005),
302 the main modification being a reduction in volume to 125 cc. Liquid volumes used in the experiments ranged from
303 20 to 50 cc, and the volumetric flow rates used ranged from 170 to 1070 ambient cc/min. Temperatures were
304 measured using a calibrated mercury thermometer, and in temperatures different than room temperatures were
305 controlled using a water bath with either ice/water, or a temperature control system. The uncertainties in the
306 temperatures were ±0.5 °C.

307 The bubble flow reactor method relies on the rapid equilibration of a gas stream that contains the analyte of
308 interest, with solution by means of the creation of small, finely divided bubbles. In the system used here, these
309 bubbles are created by passing the gas stream through a fine glass frit, situated at the bottom of the glass vessel. The
310 main sample flow is passed through the bubbler and into the detector stream to establish a baseline. A small flow of
311 the analyte is added upstream of the reactor by means of a PFA solenoid valve to start the measurement and the
312 effluent is monitored until the measured concentration attains equilibrium. At this point, the analyte entering the
313 reactor is switch off, and the concentration exiting the reactor begins to decay. This decay is due to a combination of
314 loss of the analyte as it re-equilibrates with the gas stream, and first-order loss in the solution due to reaction. Under
315 conditions of rapid equilibration, this decay takes the form of a single exponential equation, dependent on the ratio
316 of flow rate (ϕ , cm^3/s) to liquid volume (V , cm^3), the effective Henry's Law solubility H_{eff} (M/atm), and the first-
317 order loss rate (k):

$$\ln(C_0/C_t) = [\phi/(H_{\text{eff}}RTV) + k]t \quad \text{Eq. (1)}$$

321 Measurements performed at a series of ϕ/V should be linear with a slope of the decay rate ($d \ln(C_0/C_t)/dt$) vs ϕ/V of
322 $1/H_{\text{eff}}RT$, where R is the ideal gas constant, and T the temperature (K), and an x-intercept of k , the first-order loss
323 rate (s^{-1}). In practice, the linearity of this relationship and the performance of the measurement at different liquid
324 volumes and flow rates that result in the same ϕ/V provide a check on the assumption of rapid equilibration within
325 the reactor. In practice we measure the effective Henry's coefficient in our experiments, but the distinction is only
326 important for the weak acid, H₂CO₃, as described in the Results and Discussion section below.

327 Attempts to measure the solubility of ICN with the glass bubbler system described above were
328 unsuccessful, because ICN did not equilibrate at the levels and timescales typical of the other compounds measured
329 in this work, and the decay profiles were not reproducible nor exponential. The possibility that this was due to
330 higher solubility, faster reaction, or decomposition of ICN on glass surfaces was explored by using a smaller reactor
331 fabricated from 12.7 mm O.D. PFA tubing and PFA compression fittings (see supplemental Figure S1). In these
332 experiments, liquid volumes of between 1.0 and 2.0 cc and flow rates of 100 to 600 ambient cc/min were used. This
333 resulted in equilibration and decay profiles more similar to the other experiments, when the solubility of ICN in
334 water was measured at room temperature. Attempts to measure ICN solubilities in n-octanol were not successful
335 using either reactor.

336 Solution for the aqueous solubility/reaction experiments were prepared from reagent-grade materials. The
337 pH 2-4 buffer solutions were commercial preparations, made from citric acid monohydrate with differing amounts
338 of hydrochloric acid, sodium chloride, and sodium hydroxide (Fixanal, Fluka Analytical), having anion
339 concentrations ranging from 0.08 to approximately 0.2 M. The manufacturer specifications (Fluka, Sigma-Aldrich)
340 of the pH=3 buffer showed a slight temperature dependence, with the pH ranging from 3.03 at 0 °C to 2.97 at 90 °C.
341 An ammonium chloride solution of 0.45 M was prepared through addition of a measured amount of the solid to the
342 pH=3 buffer. Sodium chloride solutions ranging up to 2.5 M were prepared gravimetrically in the pH buffer

343 solution. The pHs of NH₄Cl and NaCl solutions were measured at room temperature with a pH meter and found to
344 be within 0.1 pH unit of the nominal buffer pH value.

345 III. Results and Discussion 346

347
348 Examples of the data generated by equilibration experiments are shown in Figures 1 and 2, which show the
349 exponential decays for a series of gas flow rates (Figure 1) and the correlation of the decay rates versus ϕ/V (Figure
350 2). Numerous other examples of both decay curves and decay rate versus ϕ/V are shown in the Supplementary
351 Material for a range of different analytes and solutions. The uncertainties in the Henry's coefficients are derived
352 from a combination of the reproducibility of the decay rates, the agreement between decay rates at the same ϕ/V (but
353 different flows and liquid volumes) and the fits to the slope of relationships like those shown in Figure 2, and were
354 generally $\pm 10\%$ or better. The uncertainties in first-order loss rate are the corresponding uncertainties in the
355 intercepts. The results of the experiments with HNCO, CH₃NCO, ClCN, BrCN, and ICN with the variety of solvents
356 and conditions employed are summarized in Tables 1&2 and described below.

357 358 A. Results for Aqueous Solution

359 360 1. Solubility and Reactions of HNCO 361

362 Here we report results for pHs between 2 and 4, and for the temperature range 279.5 to 310.0 K at pH=3. In
363 addition, we report data for the effect of salt concentrations on the solubility at pH=3, and the effect of ammonium
364 concentrations on solubility and apparent first-order loss rate in solution. The dependence of aqueous solubility of
365 HNCO on pH is expected given it is a weak acid, and its dissolution is accompanied by an acid-base equilibrium;



369
370 so that what is measured is the effective Henry's coefficient, H_{eff} , which involves the sum of all forms of HNCO in
371 solution:

$$373 \quad H_{\text{eff}} = \{[\text{HNCO}]_{\text{aq}} + [\text{NCO}^-]\}/[\text{HNCO}]_g \quad \text{Eq.(4)}$$

374
375 Substituting for $[\text{NCO}^-]$ using the rearranged form of Eq(3), and using Eq(2) we get the relationship for H_{eff} :

$$377 \quad H_{\text{eff}} = H(1 + K_a/[\text{H}^+]) \quad \text{Eq. (5)}$$

378
379 The plot of H_{eff} vs $1/[\text{H}^+]$ is shown in Figure 3, the slope of which is $H \times K_a$, and the intercept is the intrinsic Henry's
380 Law constant, H . The resulting fit ($R^2 = 0.99$) gave a $H = 20 (\pm 2)$ M/atm, and a K_a of $2.0 (\pm 0.3) \times 10^{-4}$ M (which

381 corresponds to $pK_a = 3.7 \pm 0.1$). The uncertainties in these numbers were derived from the standard deviations of the
382 fitted parameters, where the value for K_a is the propagated uncertainty in both H and the slope. Figure 4 shows the
383 comparison of the H measurements from this work with those of Borduas et al., (2016) plotted according to Eq. 5
384 equation. There are approximately 20% differences in the two data sets, which is just at the limits of the quoted
385 uncertainties, when both the uncertainties in the intrinsic H and pK_a are taken into account.

386 The temperature dependence of the solubility measured at $pH=3$, obeys the simple Van't Hoff relationship;
387

$$388 \quad d\ln H_{\text{eff}}/d(1/T) = -\Delta H_{\text{soln}}/R \quad \text{Eq. (6)}$$

389
390 shown in Figure 5 as a linear relationship of $\log H$ vs. $1/T$. These data were not corrected for the slight dependence
391 of the buffer pH on temperature (3.02-2.99 pH units over this range). The slope of the correlation yields a ΔH_{soln} of
392 -37.2 ± 3 kJ/mole, calculated using dimensionless Henry's coefficients ($H_{\text{eff}}RT$), (Sander, 2015). This enthalpy of
393 solution agrees with that measured by Borduas et al., (2016) (-34 ± 2 kJ/mole) within the stated uncertainties.
394 Moreover, this enthalpy is similar to those of other small N-containing molecules: HCN (-36.6 kJ/mole), CH_3CN
395 (-34.1 kJ/mole), and nitromethane (-33.3 kJ/mole) (Sander, 2015), but different than that of formic acid ($HC(O)OH$)
396 (-47.4 kJ/mole) which was used by the cloud uptake modeling study (Barth et al., 2013).

397 Often the Henry's Law solubility can depend on salt concentration of the solution, usually resulting in a
398 lower solubility (salting out), but occasionally resulting in a higher solubility (salting in), with higher salt
399 concentrations. These effects are most applicable to aerosol chemistry, where ionic strengths can be quite high. This
400 effect on HNCO solubility was measured at $pH=3$ and 298 K for NaCl solutions between 0 and 2.5 M concentration.
401 The results, shown in Figure 6, exhibit the classic "salting out" effect where HNCO was only about 60% as soluble
402 at 2.5 M compared to the standard $pH=3$ buffer. The Setschenow constant, k_s , can be determined by the relationship:
403

$$404 \quad -\text{Log}(H_{\text{eff}}/H_{\text{eff}0}) = k_s \times [I] \quad \text{Eq. (7)}$$

405
406 where H_{eff} is the Henry's coefficient at a given ionic strength, I , and $H_{\text{eff}0}$ is the Henry's coefficient in pure water.
407 For a salt with two singly charged ions, I is equal to the salt concentration. In this experiment, k_s was found to be
408 0.097 ± 0.011 M^{-1} . The magnitude of the salting out effect on HNCO is similar or slightly smaller than those found
409 for other small organic compounds in NaCl, such as acetylene, ethane and butane (Clever, 1983; Schumpe, 1993),
410 Interestingly, (Wang et al., 2014) found that Setschenow constants for ammonium sulfate $\{(NH_4)_2SO_4\}$ are typically
411 larger than those for NaCl, a feature which might impact the uptake of HNCO to aerosol particles having substantial
412 $(NH_4)_2SO_4$ content.

413 The net hydrolysis reaction rates observed in this study are listed in Table 1, and range from 0.22 to 4.15
414 $\times 10^{-3}$ s^{-1} and are both pH and temperature dependent. The main reactions of HNCO/ NCO^- in aqueous solution are
415 hydrolysis reactions that involve the acid or its conjugate anion, as detailed in Reactions 1-3 noted above. The
416 expression for the net hydrolysis reaction is;
417

418
$$k_{hydr} = \frac{k_1[H^+]^2 + k_2[H^+] + k_3K_a}{K_a + [H^+]}$$
 Eq. (8)

419
 420 as derived by Borduas et al., 2016. The rates of these reactions that were determined in several previous studies
 421 (Borduas et al., 2016; Jensen, 1958) and are in reasonable agreement except for Reaction 3, which is not
 422 atmospherically relevant. Equation 8 was used to calculate the values from those two studies that would correspond
 423 to the rates at pH=3 measured in our work, and are also listed in Table 1. The rate constants reported in this work
 424 agree within the range observed in the two previous studies, except for one temperature, and the relative standard
 425 deviations of mean values calculated from all three observations ranged from 5 to 30%.

426 The above hydrolysis reactions represent a lower limit on the condensed phase loss of HNCO, so reaction
 427 with other species present in the condensed phase might result in faster loss, and produce unique chemical species.
 428 HNCO/NCO⁻ are known to react with a variety of organic compounds having an “active hydrogen” (a hydrogen
 429 attached to an O, N, or S atom)(Belson and Strachan, 1982), through simple addition across the N=C bond, where
 430 the active hydrogen ends up on the N and the other moiety ends up attached to the carbon. For example, alcohols
 431 react to yield carbamates, i.e. esters of carbamic acid:



434
 435 Note that this is really the same mechanism as the neutral hydrolysis of HNCO, except that the addition of water
 436 forms carbamic acid, H₂NC(O)OH which is unstable and decomposes to NH₃ and CO₂. In the same fashion,
 437 HNCO/NCO⁻ can react with ammonia in solution to yield urea



440
 441 And in a more general sense, react with amines to yield substituted ureas:



444
 445 Reaction 11 is known to be an equilibrium that lies far to the product side under all conditions pertinent to this work
 446 (Hagel et al., 1971). While the forward reaction rate for R11 has been measured under neutral to slightly basic
 447 conditions (Jensen, 1959; Williams and Jencks, 1974b), it has not been measured at pHs applicable to atmospheric
 448 aerosol or cloud droplets, i.e. pH=2-4. These previous studies have assumed that the mechanism involves the
 449 reaction of the un-ionized species, e.g. NH₃ and HNCO, although there is some evidence that Reaction 12 for some
 450 amines (RNH₂) has a more complicated reaction mechanism (Williams and Jencks, 1974a). As a consequence of this
 451 assumption, the previous studies reported their reaction rates corrected for the acid-base equilibria of each species.
 452 The solubility/reaction experiment in this work was performed at pH=3 and [NH₄⁺] of 0.45 M, so a substantial
 453 correction of the literature values for the acid-base equilibria in the case of NH₄⁺ and a minor correction for the
 454 dissociation of HNCO was required in order to compare with our result. The results of our study (Table 1) show that

455 the solubility of HNCO in NH₄Cl solution at 292 K is essentially the same as that of the pH=3 buffer alone (31.5 ±3
 456 vs 32.6 ±3 M/atm). This implies that R11 does not impact the aqueous solubility. However, the measured first-order
 457 loss rate, 1.2 (±0.03) × 10⁻³ s⁻¹ is faster than the hydrolysis at pH3, 0.66 (±0.06) × 10⁻³ s⁻¹. The reaction can be
 458 expressed as the sum of hydrolysis and reactions of HNCO and NCO⁻ with NH₄⁺ (the predominant form at pH3).

$$459 \frac{d[\text{HNCO}+\text{NCO}]}{[\text{HNCO}+\text{NCO}]} = -(k_{hydr} + k_{11}[\text{NH}_4^+])dt \quad \text{Eq. (9)}$$

460 We calculate a value of 1.2 (±0.1) × 10⁻³ M⁻¹s⁻¹ for k₁₁ from our measurements which is much faster than the rate
 461 constants reported by previous studies, 5 × 10⁻⁶ M⁻¹s⁻¹ (Jensen, 1959) and 1.5 × 10⁻⁵ M⁻¹s⁻¹ (Williams and Jencks,
 462 1974b), when corrected for acid-base equilibria.

463

464 2. Solubility and Reactions of CH₃NCO

465

466 The solubility and first-order loss rate of CH₃NCO were measured at pH=2 and pH=7 at 298 K, and the
 467 results are listed in Table 1. The Henry's coefficients, 1.3 (±0.13) and 1.4 (±0.14) M/atm, were lower than those
 468 measured for HNCO, and independent of pH, within the uncertainties of the measurements. This is consistent with
 469 MIC being a less polar compound, with no dissociation reactions that might be pH dependent. In addition, these
 470 results imply that solution complexation due to the presence of anions does not affect MIC solubility, at least that
 471 the concentrations and anions present in the pH=2 buffer solution, 0.2 M for the sum of citrate and chloride.

472 The first-order loss rates of MIC, presumably due to hydrolysis, did show a pH dependence that implies
 473 acid catalysis. These hydrolysis rates were faster than the rates for HNCO at the same temperatures and pHs. The
 474 mechanism of CH₃NCO hydrolysis and other solution chemistry is discussed by (Al-Rawi and Williams, 1977;
 475 Castro et al., 1985). The hydrolysis of CH₃NCO is thought to proceed first by formation of a methyl carbamic acid:

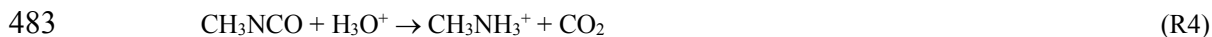
476



478

479 which is analogous to the way water adds across the N=C bond of HNCO. The methyl carbamic acid then either
 480 reacts with H₃O⁺ (faster) or H₂O (slower) to produce CH₃NH₃⁺ and CO₂, or CH₃NH₂ and CO₂, yielding the net
 481 reactions (R4) and (R5):

482



485

486 The Henry's law measurements in our work imply that if (R13) is happening, it must be to a quite minor extent,
 487 otherwise the H constant for CH₃NCO would be much larger than it is. Solution-based studies of MIC in the
 488 presence of strong acid anions (Al-Rawi and Williams, 1977; Castro et al., 1985) also imply that a complex
 489 mechanism takes place, involving a reversible complexation, (shown here for HSO₄⁻):

490



492

493 Rate constants for reactions R4 and R5 were reported by Castro et al., (1985) but the precision of these were
494 somewhat compromised by the presence of the R14 equilibrium. Again, in this study, the Henry's coefficient results
495 imply a negligible role for complexation, so the following simplified expression for the pH dependence is used:

496

$$497 \quad k_{\text{MIC}} = k_5 + k_4[\text{H}_3\text{O}^+] \quad (\text{Eq 10})$$

498

499 to derive the following values for $k_5 = 1.9 (\pm 0.6) \times 10^{-3} \text{ s}^{-1}$, and $k_4 = 0.13 (\pm 0.07) \text{ M}^{-1}\text{s}^{-1}$. These values are in
500 reasonable agreement with the value for k_5 given by Al-Rawi and Williams, (1977), $1.47 \times 10^{-3} \text{ s}^{-1}$ considering those
501 measurements were at 1M KCl, and the value for $k_4 = 0.16 \text{ M}^{-1}\text{s}^{-1}$ given by Castro et al., (1985) for reaction with
502 HCl in the absence of a buffer.

503

504 3. Solubility and Reactions of XCN Compounds.

505

506 The solubilities and first-order loss rates of XCN compounds were measured at room temperature and
507 neutral pH in pure DI water, and at ice/water temperature for ClCN and BrCN. The resulting Henry's coefficients
508 are listed in Table 2. The ClCN solubility was essentially the same as that measured for MIC at room temperature,
509 and is in reasonable agreement with the value of 0.52 M/atm at 298 K based on a model estimate (Hilal et al., 2008),
510 and one reported measurement, 0.6 M/atm at 293 K (Weng et al., 2011). In contrast, BrCN was more soluble than
511 ClCN, $8.2 \pm 0.8 \text{ M/atm}$ at 296°K, but fairly insoluble in an absolute sense. The temperature dependences of H_{ClCN}
512 and H_{BrCN} were as expected, showing higher solubility at lower temperatures, however, they had very different heats
513 of solution, -27.8 kJ/mole for ClCN, and -38.3 kJ/ mole for BrCN, although there are only two data points for each
514 compound. Both the higher solubilities and larger ΔH_{soln} , could be a result of the higher dipole moment and
515 polarizability of BrCN relative to ClCN (Maroulis and Pouchan, 1997).

516 The solubility of ICN was measured a room temperature using a combination of different flow rates (208 –
517 760 amb cm^3/min) and liquid volumes (1.95 and 0.95cc). A plot of the decay rates versus ϕ/V for those runs is
518 shown in Figure 7. Where those data sets overlap there is agreement to within about 15%, implying that the
519 equilibration could be fast enough to meet the criteria for these types of flow experiments. The resulting Henry's
520 coefficient, $270 (\pm 41) \text{ M/atm}$ is significantly larger than the other two XCN compounds, but is consist with the trend
521 of increasing solubility with dipole moment and polarizability. Attempts to use the small reactor to measure the
522 solubility of ICN at ice/water temperatures was not successful, e.g. did not yield simple single exponential decays
523 with time under the same range of flow conditions as used in the room temperature experiment.

524 The hydrolysis of XCN compounds is known to be base-catalyzed, and can be susceptible to anion
525 complexation (Bailey and Bishop, 1973; Gerritsen et al., 1993) in a manner similar to MIC:

526





530
531 This complexation can be ignored in our study for ClCN and BrCN since the experiment was performed in
532 DI water, however, such complexation should be considered in future condensed phase studies of XCN compounds.
533 Accordingly, the expression for the ClCN and BrCN hydrolysis rate constant is;

534
535 $k_{\text{XCN}} = k_w + k_{\text{OH}}[\text{OH}^-]$ (Eq.11)

536
537 Bailey and Bishop (1973) found $k_w = 2.58 \times 10^{-6} \text{ s}^{-1}$ and $k_{\text{OH}} = 4.53 \text{ M}^{-1}\text{s}^{-1}$ at 299.7 K, for ClCN, which corresponds
538 to 3.03×10^{-6} at pH7. This is consistent with the results of this study which found that the first-order loss rate was
539 zero, within the error of the linear fit ($\pm 4.2 \times 10^{-4} \text{ s}^{-1}$). The study of BrCN hydrolysis of Gerritsen et al., 1993 did not
540 derive k_w nor did it present sufficient data for k_w to be estimated. However, there are two other studies that presented
541 data from which k_w can be estimated, and those range from $1.9 - 9.2 \times 10^{-5} \text{ s}^{-1}$, (Heller-Grossman et al., 1999;
542 Vanelslander et al., 2012).

543 The hydrolysis of ICN is slightly more complicated since there is some evidence that ICN might complex
544 with iodide (Gerritsen et al., 1993). The room temperature hydrolysis rate observed in our experiment was not
545 significantly different than zero, $4.4 (\pm 7.6) \times 10^{-5} \text{ s}^{-1}$, but is in the same range of the rate constant estimated from the
546 data given by Gerritsen, et al., (1993), by extrapolating their rate constant vs. $[\text{OH}^-]$ data to zero $[\text{OH}^-]$, assuming no
547 complexation reactions.

548 549 B. Non-aqueous Solution

550
551 Solubility in non-aqueous solvents is a standard indicator of how compounds will be distributed between
552 different compartments in the environment, i.e. lipids in the body, organic aerosols in the atmosphere. In addition,
553 the ratio of organic to aqueous solubility (K_{ow}) is used to estimate membrane transport of a chemical species, a key
554 factor in estimating physiologic effects of a pollutant. Several non-aqueous solvents were used in this study,
555 tridecane to represent a completely non-polar solvent and n-octanol, which is used as a standard material for such
556 studies. Tridecane was used because it is the heaviest n-alkane that is still a liquid at 273.15K, and it has purely non-
557 polar character, i.e. no functional groups, so is a slightly different model for non-polar matrices.

558 559 1. Solubility and Reactions of HNCO

560
561 The experiments performed on HNCO were conducted with tridecane, 10% (V/V) n-octanol/tridecane, and
562 pure n-octanol, and the results are summarized in Table 1. HNCO is the least soluble in tridecane, $1.7 (\pm 0.17) \text{ M/atm}$
563 and increasingly soluble as the proportion of n-octanol is increased, to pure n-octanol, $87 (\pm 9) \text{ M/atm}$ at 298 K.
564 Experiments at two other temperatures were performed to confirm that these solubilities follow the expected
565 temperature dependence, and to obtain the solubility in pure n-octanol at human body temperature (310 K) to match

566 data for the aqueous solubility. The lower solubility of HNCO in tridecane is expected since tridecane is completely
567 non-polar and has no tendency to hydrogen bond or interact with the polarizable end of the HNCO molecule. In
568 contrast, the increase in solubility of HNCO with increasing proportion of n-octanol is due to the polar -OH group at
569 the end of the molecule.

570 The rate of reactions of HNCO with the non-aqueous solvents were below the limit of detection by this
571 method for all combinations except for pure n-octanol at 310 K. Even still, the measured rate was quite a bit lower
572 than the corresponding hydrolysis rate in aqueous solution at pH=3. The manner in which these two factors
573 (solubility and reaction) affect the net uptake and loss of HNCO will be discussed below.

574

575 2. Solubility and Reactions of CH₃NCO

576

577 The solubility of CH₃NCO in n-octanol was measured at several temperatures, as summarized in Table 1. The
578 value for 298 K is approximately 3 times higher than that of aqueous solubility, and has the expected temperature
579 dependence. In addition, the first-order reaction rates for CH₃NCO in n-octanol were in the same range or slightly
580 higher than the aqueous reactions. The reaction with n-octanol is expected to go via the carbamylation reaction
581 (R10), although there is some evidence that this reaction has a more complex mechanism possibly involving
582 multiple alcohol molecules (Raspoet et al., 1998). These rates are much faster than the corresponding rates for
583 HNCO, and may provide some guidance concerning the loss rates of CH₃NCO to heterogeneous processes.

584

585 3. ClCN and BrCN

586

587 The solubilities of ClCN and BrCN in n-octanol were measured at room temperature. Cyanogen chloride and
588 BrCN have about the same relative differences in solubility in n-octanol (a factor of 3-4) as they did H₂O. The higher
589 solubility of BrCN relative to ClCN could again be due to its higher dipole moment and polarizability (Maroulis and
590 Pouchan, 1997). The first-order loss rates of ClCN and BrCN could be determined from the flow reactor experiments
591 and were $1.3 (\pm 0.4) \times 10^{-3} \text{ s}^{-1}$ and $9 (\pm 2) \times 10^{-5} \text{ s}^{-1}$, respectively. Reactions of ClCN with alcohols are known (see for
592 example (Fuks and Hartemink, 1973)), and form carbamates, in a mechanism that appears to be second-order in the
593 alcohol, and acid catalyzed, but rate constants for ClCN-alcohol reactions have not been reported to our knowledge.
594 There are studies of rates of reactions of ClCN with nucleophiles, e.g. nitrogen bases, and those reactions appear to
595 result in -CN substitution and formation of a Cl⁻ ion (Edwards et al., 1986). In addition, BrCN has been used by
596 protein chemists to selectively cleave disulfide bonds and has been used for some time by synthetic chemists to
597 selectively convert tertiary amines to secondary amines (Siddiqui and Siddiqui, 1980; von Braun and Schwarz, 1902)
598 and can carbamylate amino acids (Schreiber and Witkop, 1964). The importance of these reactions to the atmospheric
599 fate of XCN compounds remains an open question, but it is important to note that they constitute losses of active
600 halogen, i.e. conversion of the halogen to a halide ion.

601

602 4. Octanol/Water Partition Coefficients

603
604 The ratio of solubilities between a non-polar solvent and water is a fundamental quantity that is useful in
605 predicting the fate of a compound in the environment and biological systems (Leo et al., 1971). This parameter is
606 used to predict lipid solubility, membrane transport, and the potential of uptake of a particular compound by organic
607 aerosol. n-Octanol is a standard non-polar solvent that is commonly used for this purpose, as it has an overall non-
608 polar character with a substituent that is capable of hydrogen bonding. The data from this study can be used to
609 calculate the octanol/water partition coefficients for HNCO, CH₃NCO, ClCN, and BrCN as the ratio of the
610 respective Henry's coefficients;

$$611 \quad K_{ow} = H_{oct}/H_{H_2O} \quad (Eq.12)$$

612 The results are listed in Table 4 along with K_{ow}s for some related small molecules. Both CH₃NCO, and BrCN are
613 fundamentally more soluble in n-octanol than in water, while ClCN has nearly the same solubility in both materials.
614 The weak acid equilibrium of HNCO makes it more soluble in n-octanol at pH 3, but much more soluble in water at
615 neutral pH. However, transport models of biological systems account for these acid base equilibria along with using
616 the K_{ow} to estimate transport rates (Missner and Pohl, 2009). Formic acid is a similarly weak acid (pK_a = 3.77) and
617 so is a good point of comparison to HNCO. The n-octanol partition coefficient of HNCO is a factor of 15 larger than
618 that of HC(O)OH, so should have larger membrane permeabilities. Similarly, the n-octanol partition coefficient of
619 CH₃NCO is 6.8 times larger than that of CH₃CN. The two cyanogen halides measured here had differing behavior,
620 with ClCN showing almost no difference in solubility, and BrCN having about the same increase in solubility in n-
621 octanol as HNCO and CH₃NCO.

622 623 **IV. Atmospheric and Environmental Chemistry Implications** 624

625 The atmospheric loss of the compounds studied here are either solely or predominantly through
626 heterogeneous uptake and reaction for HNCO, CH₃NCO, ClCN, BrCN, or in the case of ICN due to both
627 heterogeneous chemistry and photolysis. The aqueous solubility and reaction data from this study allow some
628 prediction of uptake parameters and loss rates in some important systems, e.g. cloud water and natural water
629 surfaces like oceans. In addition, some indications can be gained about the uptake of HNCO, CH₃NCO, ClCN, and
630 BrCN to organic aerosol, using n-octanol as a model. Finally, the n-octanol/water partition coefficient is often used
631 as a key parameter in modeling cross-membrane transport, and the data from this study can be used to predict the
632 behavior of these reduced-N compounds relative to other well-studied compounds.

633 The reactive uptake of HNCO, CH₃NCO and XCN on environmental surfaces, small particles and aqueous
634 droplets can be parameterized using the uptake coefficient, γ , defined as the fraction of collisions of a molecule with
635 a surface that lead to incorporation of that molecule in the condensed phase. If solubility and reaction are the
636 limiting processes, a good assumption for the species in this work, then γ_{rxn} can be estimated from the following
637 equation (Kolb et al., 1995):

$$638 \quad \gamma_{rxn} = \frac{4HRT\sqrt{kD_a}}{\langle c \rangle} \quad (Eq.13)$$

639 where H and k are the Henry's coefficient and first-order loss rate in solution measured in this work, R is the gas
 640 constant, T is temperature, D_a is the diffusion coefficient in aqueous solution (assumed here to be $1.9 \times 10^{-5} \text{ cm}^2 \text{ s}^{-1}$
 641 for HNCO and $1.6 \times 10^{-5} \text{ cm}^2 \text{ s}^{-1}$ for CH_3NCO and ClCN, $1.2 \times 10^{-5} \text{ cm}^2 \text{ s}^{-1}$ for BrCN, and $1.0 \times 10^{-5} \text{ cm}^2 \text{ s}^{-1}$ for ICN at
 642 298 K), and $\langle c \rangle$ is the mean molecular velocity. The results of these calculations are shown in Figure 8 for the H
 643 measurements at 298K reported here, k_{hydr} for HNCO reported by Borduas et al., (2016), k_{hydr} for CH_3NCO from this
 644 work and k_{hydr} for ClCN from Bailey and Bishop (1973).

645 Deposition of a compound to the surface can be parameterized as essentially two processes taking place in
 646 series, physical transport within the planetary boundary layer to the surface and then chemical uptake on the surface
 647 (see for example (Cano-Ruiz et al., 1993)). In this formulation, the deposition velocity, v_d (the inverse of the total
 648 resistance) is expressed as follows:

$$649 \quad v_d = \frac{1}{\frac{1}{v_t} + \frac{1}{\frac{\gamma \langle c \rangle}{4}}} \quad (\text{Eq.14})$$

650 where $1/v_t$ is the resistance due to transport, and $\frac{1}{\frac{\gamma \langle c \rangle}{4}}$ is the resistance due to chemical uptake. For a species for
 651 which uptake is rapid, e.g. a highly soluble acid, the chemical resistance becomes small and $v_d \cong v_t$. This is the case
 652 for HNCO deposition to land or natural water surfaces (pHs ~ 7 -8). Typical v_t s are on the order of 0.5 to 1 cm/s for a
 653 reasonably mixed boundary layer (Wesely and Hicks, 2000). For compounds for which γ is quite small, the
 654 chemical term predominates.

$$655 \quad v_d \cong \frac{\gamma \langle c \rangle}{4} \quad (\text{Eq.15})$$

656 The lifetime of a species within the PBL then can be estimated as h/v_d , where h is the boundary layer height. The
 657 lifetime estimates for HNCO, CH_3NCO , and XCN compounds are given in Table 3, and range from the short
 658 lifetime noted for HNCO, to quite long lifetimes for the least soluble species, for example ClCN.

659 The loss rates due to uptake of species to atmospheric aerosol particles can be estimated from the pH
 660 dependent uptake coefficients in Figure 8, using parameterizations described in the literature (Davidovits et al.,
 661 2006; Sander, 1999). In the limited case of surface-controlled uptake, i.e. neglecting gas phase diffusion, the loss of
 662 a species is;

$$663 \quad k = \frac{A \gamma \langle c \rangle}{4} \quad (\text{Eq.16})$$

664 where A is the aerosol surface area. If we take the γ s from Figure 8, and assume highly polluted conditions to obtain
 665 a lower limit to the lifetime against this process, $A = 1000 \mu\text{m}^2/\text{cm}^3$ and pHs between 1 and 2, then the lifetimes
 666 listed in Table 3 are arrived at. The values for HNCO and CH_3NCO show a range because the uptake is pH
 667 dependent, and it should be noted that the values for CH_3NCO , ClCN, and BrCN are over estimated by this method,
 668 as their chemistry is slow enough that a volume-based estimate may be more appropriate. The more important effect
 669 here is that the γ values are based on hydrolysis losses, which are undoubtedly much slower than many of the solution-
 670 phase reactions that these species can undergo, hence the lifetimes against aerosol deposition are upper limits.
 671
 672

673 The loss of HNCO to cloudwater is the subject of extensive work discussed by Barth et al, (2013), and no
674 attempt will be made here to update that analysis. We can point out that our results yielded slightly lower H_{eff}
675 ($\sim 22\%$) at the lowest temperature we measured, compared to the values used by Barth et al., (2013), see Figure S13.
676 This would result in slightly slower removal rates in the Barth et al., model in low-temperature clouds. The fastest
677 loss rates for HNCO were observed in warm dense clouds into which SO_2 was also dissolving and adding
678 considerable acidity, so that value for HNCO was included in Table 3. For the other compounds we use a simple
679 parameterization of cloudwater reaction to estimate the in-cloud loss rates for CH_3NCO and the XCN compounds. In
680 the estimate of reaction rate:

$$681 \quad k = k_l L_c \text{HRT} \quad (\text{Eq. 17})$$

682 k_l is the liquid phase rate constant, L_c is the cloud liquid water content, and H is the Henry's coefficient. If we
683 assume a L_c of 2×10^{-6} , and $T \cong 298 \text{ K}$, and we use the H and k values measured in this work (the exception is that
684 the literature value for CH_3NCO at $\text{pH}=2$ was used), then the values for lifetimes of CH_3NCO , and XCN compounds
685 listed in Table 3 were obtained. Below we discuss the characteristic times obtained for each compound in the
686 context of what else is known about their sources and atmospheric chemistry.

687 A. HNCO

688 The loss of HNCO via heterogeneous processes occurs in two separate regimes: in aerosols and cloud
689 droplets at relatively low pH, and in surface waters and on terrestrial surfaces that are neutral or slightly basic in pH.
690 In the former case, HNCO solubility is relatively low but hydrolysis is acid catalyzed. In the latter case, solubility is
691 high enough that uptake will be limited by the transport of HNCO to the surface, much like other strong acids such
692 as HNO_3 . Ambient measurements of HNCO at surface sites are consistent with deposition of HNCO to the ground,
693 exhibiting diurnal profiles similar to those of O_3 or HNO_3 (Kumar et al., 2018; Roberts et al., 2014; Mattila, et al.,
694 2018; Zhao et al., 2014).

695 Several aspects of the aqueous solubility and hydrolysis, and heterogeneous removal of HNCO have been
696 examined in modeling studies. A global modeling study by Young et al. (2012) was a first attempt to model global
697 HNCO by scaling the source to fire emissions of HCN. Loss of HNCO was assumed to be due to wet and dry
698 deposition with efficiencies similar to HNO_3 and HC(O)OH , and that HNCO was lost once it was taken up by
699 clouds. Young et al., concluded that HNCO had an average lifetime of about 37 days. Barth et al., (2013) addressed
700 part of this analysis by modeling the cloud removal of HNCO using actual solubility and reaction data in a cloud
701 parcel model, albeit, the hydrolysis rates used were from Jensen, (1957) which were approximately 50% higher than
702 the Borduas results, and the temperature dependence of H_{eff} was assumed equal to that of HC(O)OH , and resulted in
703 higher solubilities at low temperature. This cloud model showed that cloud water uptake was reversible in that most
704 cases hydrolysis was slow enough that some HNCO returned to the gas phase after cloud evaporation. The Barth et
705 al., study estimated HNCO lifetimes as short as 1 hour in warm polluted clouds (i.e. high $\text{SO}_2 \Rightarrow \text{H}_2\text{SO}_4$ formation).
706 The results of our study and those of Borduas et al., (2016) add to these analyses in that now the measured
707 temperature dependence of H_{eff} can be used, and the hydrolysis rate constants can be updated.
708
709

710 The results in this paper allow for further refinement of HNCO loss estimates. For example, the salting-out
711 effect may be important for aerosol with high inorganic content, and high ammonium concentrations will result in
712 reactive loss rates that are faster than hydrolysis. The solubility of HNCO in aerosol particles with substantial
713 organic character can be higher or low depending on the nature of substituent groups, e.g. degree of -OH
714 functionalization. Given that aerosol particles in most polluted atmospheres are at least half organic carbon by mass
715 (Jimenez and et al., 2009), it is useful to estimate what effect an increased solubility of HNCO might have on its
716 removal lifetime. If take our $1000 \mu\text{m}^2/\text{cm}^3$ surface area aerosol from the above calculation, assume a 50/50 organic
717 to aqueous distribution and that the solubility of HNCO in the organic fraction is the same as n-octanol, we can
718 arrive at a weighted average Henry's solubility of 55 M/atm. If we combine that with the same reaction rate
719 corresponding to pH1, then the lifetime of HNCO against reaction to this aerosol drops to about 2 days, a significant
720 effect.

721 In studies of the condensed phase oxidation of dissolved N species, as well as biological processes produce
722 cyanate ion, there is a growing recognition that cyanate is part of the natural N cycle in the ocean (see (Widner et al.,
723 2013) and references there-in). Observed near-surface cyanate levels often reached a few 10s of nM in near shore
724 productive areas. The observations of cloud/aerosol source of HNCO presented in (Zhao et al., 2014) on the coast
725 of California might be explained by a combination of this NCO^- seawater source and aerosol/cloud water
726 acidification by local sources of strong acids, particularly HNO_3 . In specific, acidification of sea spray containing
727 about 10 nM NCO^- to pH=4 or so, would correspond to H_{eff} of around 50 M/atm, and result in an equilibrium
728 HNCO concentration of several hundred pptv. Such a source would most likely be limited by the concentration of
729 sea salt-derived aerosol, but could easily account for the source implied by the measurements of (Zhao et al., 2014).

730 731 B. CH_3NCO

732 The atmospheric chemistry of CH_3NCO is less well studied than HNCO. There is a single reported
733 measurement of the reaction rate of CH_3NCO with OH by relative rates which gave $k = 3.6 \times 10^{-12} \text{ cm}^3 \text{ molec}^{-1} \text{ s}^{-1}$
734 (Lu et al., 2014), however recent work indicates that secondary chemistry may have made this rate high by a
735 significant amount (Papanastasiou, et al., manuscript in preparation, 2019). In addition, there are likely condensed-
736 phase reactions that are faster than the simple hydrolysis reactions consider in this work. Never-the-less, it is useful
737 to estimate the atmospheric loss rates implied by our work, as a baseline against which future atmosphere
738 observations can be judged, and the importance of other heterogeneous processes can be assessed. The uptake
739 coefficients estimated for CH_3NCO in Figure 8 are relatively low with only a slight increase at the lowest pHs in
740 atmospheric media. As a consequence, atmospheric lifetimes of CH_3NCO towards surface deposition are estimated
741 to be quite long, 6 months or more if hydrolysis is the sole loss process. The loss due to aerosol or cloudwater
742 uptake is estimated to be slightly faster, due primarily to the slight acid-catalysis of the CH_3NCO hydrolysis rate.

743 744 C. ClCN , BrCN , and ICN

745
746 To date, we know of no observations of ClCN in the ambient atmosphere, but its formation in the
747 chlorination of water, waste water, and swimming pools (Afifi and Blatchley III, 2015; Daiber et al., 2016; Lee et
748 al., 2006) indicates that there could be sources from human activities, including the use of chlorine bleach for

749 cleaning indoor surfaces. In addition, there might also be a source from aerosol systems where chlorine is being
750 activated, i.e. oxidized from Cl^- to ClNO_2 , Cl_2 , or HOCl (see for example (Roberts et al., 2008)) in the presence of
751 reduced nitrogen. The results of our solubility measurements indicate that ClCN will volatilize from the condensed
752 phase fairly readily, e.g. within seconds of the application of a thin film of chlorine bleach cleaning solution, or the
753 bubbling of air through a spa in which ClCN is dissolved. As a result, the atmospheric removal of ClCN should be
754 considered. BrCN has been observed in systems where bromide-containing water or wastewater were treated with
755 halogens (Heller-Grossman et al., 1999), and there are biological mechanisms that make BrCN and ICN as well
756 (Schlorke et al., 2016; Vanelslander et al., 2012). The potential for remote atmospheric sources of these compounds
757 is currently being investigated, but BrCN could be the result of the same bromine activation chemistry that depletes
758 ground level ozone in that environment (Simpson et al., 2007).

759 Gas phase radical reactions of XCN compounds have not been studied under atmospheric conditions. A few
760 studies at higher temperatures and the studies of HCN and CH_3CN can be used to roughly predict how fast the
761 relevant reactions are. For example, the reactions of ClCN and BrCN with O atoms at 518-635 K are very slow (<3
762 $\times 10^{-15} \text{ cm}^3 \text{ molec}^{-1} \text{ s}^{-1}$, (Davies and Thrush, 1968)) and the reaction of Cl atom with ClCN at high temperature is also
763 quite slow ($<1.0 \times 10^{-14} \text{ cm}^3 \text{ molec}^{-1} \text{ s}^{-1}$, (Schofield et al., 1965)). However, these observations do not preclude the
764 presence of another reaction channel at low temperature, e.g. a mechanism involving addition to the CN group. The
765 reactions of HCN and CH_3CN with OH , Cl atom and O atom at atmospherically relevant temperatures are all quite
766 slow, implying such addition channels are not likely to be substantially faster for these XCN compounds. We
767 conclude that rate constants for the reactions of OH or Cl with X-CN compounds are likely quite low ($<2 \times 10^{-14} \text{ cm}^3$
768 $\text{ molec}^{-1} \text{ s}^{-1}$), making the lifetimes of these compounds against these reactions on the order of a year or longer. The
769 UV-visible absorption spectra of all three of these compounds have been measured (Barts and Halpern, 1989; Felps
770 et al., 1991; Hess and Leone, 1987; Russell et al., 1987), have maxima that range from $<200\text{nm}$ for ClCN , 202nm
771 for BrCN , and 250nm for ICN , with absorption that tails into near-UV and visible wavelengths, (see Figure S13 in
772 the Supplemental Material). Extrapolation of the spectra, combined with photo fluxes estimated from the NCAR
773 TUV model for mid-summer 40° North at the surface, result in a range of photolysis behavior ranging from no
774 tropospheric photolysis of ClCN , to slight photolysis of BrCN ($\tau \cong 135$ days), and faster photolysis of ICN ($\tau \cong 9$
775 hours). The above gas phase processes provide the context in which to assess the importance of condensed phase
776 loss processes of ClCN , BrCN , and ICN . Rates of loss of XCN compounds due to surface deposition, cloudwater or
777 aerosol uptake would need to be faster than the gas phase processes to be important in the atmosphere. In addition,
778 condensed phase reactions convert XCN to halide ions either by hydrolysis to cyanate, or creation of a carbamyl
779 functionalities. Only photolysis reforms the halogen atom, and therefore maintains active halogen reaction chain.
780 Estimated atmospheric lifetimes of XCN compounds against loss due to condensed phase reactions listed in Table 3
781 shows a general trend. The lifetimes become shorter as the halogen atom goes from Cl to Br to ICN , primarily due to
782 higher solubilities. The actual condensed phase losses are likely much shorter than those estimated here because of
783 faster condensed phase reactions that are not taken into account by the brief analysis presented here. Depending on
784 the mechanism of condensed phase XCN reactions, this chemistry could be a condensed phase source of NCO^- and
785 therefore HNCO similar that observed by Zhao et al. (2014) in coastal clouds.

786

787 D. Solubility in non-polar media, uptake to organic aerosol, and membrane transport.

788

789 The solubilities of HNCO, CH₃NCO, and BrCN in n-octanol were roughly a factor 4 larger than water,
790 while that of ClCN was virtually the same. Reaction rates with n-octanol were the same or slower than for aqueous
791 solutions, except for ClCN which was faster than hydrolysis at pH=7. As a result, loss due to uptake to organic
792 aerosol will be only slightly faster for all of these species. Membrane transport is a key process in determining the
793 extent to which a chemical species will impact biological systems. Simple membrane transport models parameterize
794 this process as diffusion through a lipid bi-layer according to a partition coefficient, K_p , which the ratio of
795 solubilities in lipid versus aqueous media (Missner and Pohl, 2009), and K_{ow} is often used for this partition
796 coefficient. The results of our work indicate that both HNCO and CH₃NCO are more soluble in n-octanol than
797 water, in contrast to other similar small organic acids and N-containing compounds (Table 4). These features will
798 need to be accounted for in assessing the connection by between environmental exposure to HNCO, CH₃NCO,
799 ClCN and BrCN and resulting biochemical effects.

800

801 **V. Data availability.** The data are available on request.

802

803 **VI. Author contributions.** YL and JR performed the laboratory experiments and JR and YL wrote the paper.

804

805 **VII. Competing interests.** The author declare no competing interests.

806

807 **VIII. Disclaimer.** Any mention of commercial products or brands were solely for identifying purposes and should
808 not be construed as an endorsement.

809

810 **IX. Acknowledgements**

811

812 We thank Drs. James B. Burkholder, François Bernard, for help with the FTIR analysis and Drs. Patrick
813 Veres and Bin Yuan for the CIMS analyses of XCN samples. We thank Dr. Dimitris Papanastasiou, Dr. J. Andrew
814 Neuman, and Dr. Patrick Veres for communicating the results of their work prior to publication. This work was
815 supported in part by NOAA's Climate and Health of the Atmosphere Initiatives.

816

817

818 **X. References**

819

820

821 Afifi, M. Z. and Blatchley III, E. R.: Seasonal dynamics of water and air chemistry in an indoor chlorinated
822 swimming pool, *Water Res.*, 68, 771-783, 2015.

823

824 Al-Rawi, H. and Williams, A.: Elimination-addition mechanisms of acyl group transfer: the hydrolysis and synthesis
825 of carbamates, *J. Am. Chem. Soc.*, 99, 2671-2678, 1977.

826

827 Bailey, P. L. and Bishop, E.: Hydrolysis of cyanogen chloride, *J. Chem. Soc., Dalton Trans.*, doi:
828 10.1039/dt9730000912, 1973. 912-916, 1973.

829

830 Barnes, I., Solignac, G., Mellouki, A., and Becker, K. H.: Aspects of the atmospheric chemistry of amides, *Chem*
831 *Phys Chem*, 11, 3844-3857, 2010.
832
833 Barth, M. C., Cochran, A. C., Fiddler, M. N., Roberts, J. M., and Bililign, S.: Numerical modeling of cloud
834 chemistry effects on isocyanic acid (HNCO), *J. Geophys. Res.*, 118, 2013.
835
836 Barts, S. A. and Halpern, J. B.: Photodissociation of ClCN between 190 and 213 nm, *J. Phys. Chem.*, 93, 7346-7351,
837 1989.
838
839 Belson, D. J. and Strachan, A. N.: Preparation and properties of isocyanic acid, *Chem. Soc. Rev.*, 11, 41-56, 1982.
840
841 Bengtstrom, L., Salden, M., and Stec, A. A.: The role of isocyanates in fire toxicity, *Fire Sci. Rev.*, 5, 1-23, 2016.
842
843 Blomqvist, P., Hertzberg, T., Dalene, M., and Skarping, G.: Isocyanates, aminoisocyanates, and amines from fires -
844 a screening of common materials found in buildings, *Fire Mater.*, 27, 275-294, 2003.
845
846 Boenig, D. W. and Chew, C. M.: A critical review: general toxicity and environmental fate of three aqueous cyanide
847 ions and associated ligands, *Water, Air and Soil Pollut.*, 109, 67-79, 1999.
848
849 Borduas, N., da Silva, G., Murphy, J. G., and Abbatt, J. P. D.: Experimental and theoretical understanding of the gas
850 phase oxidation of atmospheric amides with OH radicals: Kinetics, products, and mechanisms, *J. Phys. Chem. A*,
851 119, 4298-4308, 2015.
852
853 Borduas, N., Place, B., Wentworth, G. R., Abbatt, J. P. D., and Murphy, J. G.: Solubility and reactivity of HNCO in
854 water: insights into HNCO's fate in the atmosphere, *Atmos. Chem. Phys.*, 16, 703-714, 2016.
855
856 Broughton, E.: The Bhopal disaster and its aftermath: a review, *Environ. Health*, 4, 6-12, 2005.
857
858 Bunkan, A. J. C., Hetzler, J., Mikoviny, T., Wisthaler, A., Nielsen, C. J., and Olzmann, M.: The reactions of N-
859 methylformamide and N,N-dimethylformamide with OH and their photo-oxidation under atmospheric conditions:
860 experimental and theoretical studies, *Phys. Chem. Chem. Phys.*, 17, 7046-7059, 2015.
861
862 Cano-Ruiz, J. A., Kong, D., Balas, R. B., and Nazaroff, W. W.: Removal of reactive gases at indoor surfaces:
863 Combining mass transport and surface kinetics *Atmos. Environ.*, 27A, 2039-2050, 1993.
864
865 Castro, E. A., Moodie, R. B., and Sansom, P. J.: The kinetics of hydrolysis of methyl and phenyl isocyanates, *J.*
866 *Chem. Soc. Perkin Trans II*, 2, 737-742, 1985.
867
868 Chandra, B. P. and Sinha, V.: Contribution of post-harvest agricultural paddy residue fires in the N.W. Indo-
869 Gangetic Plain to ambient carcinogenic benzenoids, toxic isocyanic acid and carbon monoxide, *Environ. Intl.*, 88,
870 187-197, 2016.
871
872 Clever, H. L.: Sechenov salt-effect parameter, *J. Chem. Eng. Data*, 28, 340-343, 1983.
873
874 Daiber, E. J., DeMarini, D. M., Ravuri, S. A., Liberatore, H. K., Cuthbertson, A. A., Thompson-Klemish, A., Byer,
875 J. D., Schmid, J. E., Afifi, M. Z., Blatchley III, E. R., and Richardson, S. D.: Progressive increase in disinfection
876 byproducts and mutagenicity from source to tap to swimming pool and spa water: Impact of human inputs, *Environ.*
877 *Sci. Technol.*, 50, 6652-6662, 2016.
878
879 Davidovits, P., Kolb, C. E., Williams, L. R., Jayne, J. T., and Worsnop, D. R.: Mass accommodation and chemical
880 reactions at gas-liquid interfaces, *Chemical Reviews*, 106, 1323-1354, 2006.
881
882 Davies, P. B. and Thrush, B. A.: Reactions of oxygen atoms with hydrogen cyanide, cyanogen chloride and
883 cyanogen bromide, *Trans. Faraday Soc.*, 64, 1836-1843, 1968.
884

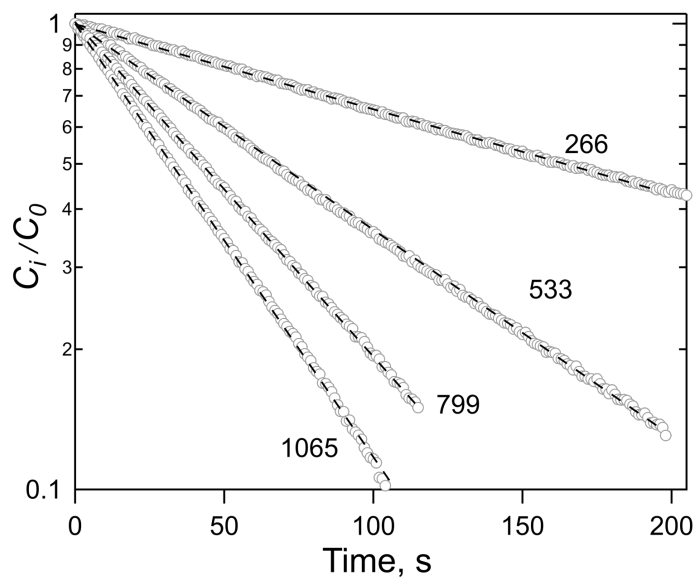
885 Davis, D. D. and Okabe, H.: Determination of bond dissociation energies in hydrogen cyanide, cyanogen and
886 cyanogen halides by the photodissociation method., *J. Chem. Phys.*, 49, 5526-5531, 1968.
887
888 Diehl, A. C., Speitel Jr., G. E., Symons, J. M., Krasner, S. W., Hwang, C. J., and Barrett, S. E.: DBP formation
889 during chloramination, *J. Am. Water Works Assoc.*, 92, 76-90, 2000.
890
891 Edwards, J. O., Erstfeld, T. E., Ibne-Rasa, K. M., Levey, G., and Moyer, M.: Reaction rates for nucleophiles with
892 cyanogen chloride: Comparison with two other digonal carbon compounds, *Int. J. Chem. Kinet.*, 18, 165-180, 1986.
893
894 Epstein, J.: Estimation of microquantities of cyanide, *Anal. Chem.*, 19, 272-274, 1947.
895
896 Felps, W. S., Rupnik, K., and McGlynn, S. P.: Electronic spectroscopy of the cyanogen halides. , *J. Phys. Chem.*, 95,
897 639-656, 1991.
898
899 Fuks, R. and Hartemink, M. A.: The acid-catalyzed reaction of cyanogen chloride with aliphatic alcohols. A general
900 synthesis of aliphatic carbamates, *Bulletin des Societes Chimiques Belges*, 82, 23-30, 1973.
901
902 Garrido, M. A., Gerecke, A. C., Heeb, N., Font, R., and Conesa, J. A.: Isocyanate emissions from pyrolysis of
903 mattresses containing polyurethane foam, *Chemosphere*, 168, 667-675, 2017.
904
905 Geddes, J. D., Miller, G. C., and Taylor Jr., G. E.: Gas phase photolysis of methyl isothiocyanate, *Environ. Sci.*
906 *Technol.*, 29, 2590-2594, 1995.
907
908 Gerritsen, C. M., Gazda, M., and Margerum, D. W.: Non-metal redox kinetics: Hypobromite and hypiodite
909 reactions with cyanide and the hydrolysis of cyanogen halides, *Inorg. Chem.*, 32, 5739-5748, 1993.
910
911 Goesmann, F., Rosenbauer, H., Bredehoft, J. H., Cabane, M., Ehrenfreund, P., Gautier, T., Giri, C., Kruger, H., Le
912 Roy, L., MacDermott, A. J., McKenna-Lawlor, S., Meierhenrich, U. J., Munoz Caro, G. M., Raulin, F., Roll, R.,
913 Steele, A., Steininger, H., Sternberg, R., Szopa, C., Thiemann, W., and Ulamec, S.: Organic compounds on comet
914 67P/Churyumov-Gerasimenko revealed by COSAC mass spectrometry, *Science*, 349, aab0689-0681,0683, 2015.
915
916 Hagel, P., Gerding, J. J. T., Fieggen, W., and Bloemendal, H.: Cyanate formation in solutions of urea .I. Calculation
917 of cyanate concentrations at different temperature and pH, *Biochimica et Biophysica Acta*, 243, 366, 1971.
918
919 Halfen, D. T., Ilyushin, V. V., and Ziurys, L. M.: Interstellar detection of methyl isocyanate CH₃NCO in Sgr B2(N):
920 A link from molecular clouds to comets, *Astrophysical Journal Letters*, 812, L5, 2015.
921
922 Hardy, J. E. and Knarr, J. J.: Technique for measuring the total concentration of gaseous fixed nitrogen species, *J. Air*
923 *Pollut. Contr. Assoc.*, 32, 376-379, 1982.
924
925 Heller-Grossman, L., Idin, A., Limoni-Relis, B., and Rebhun, M.: Formation of cyanogen bromide and other volatile
926 DBPs in the disinfection of bromide-rich lake water., *Environ. Sci. Technol.*, 33, 932-937, 1999.
927
928 Hess, W. P. and Leone, S. R.: Absolute I* quantum yields for the ICN \tilde{A} state by diode laser gain-vs-absorption
929 spectroscopy, *J. Chem. Phys.*, 86, 3773-3780, 1987.
930
931 Hilal, S. H., Ayyampalayam, S. N., and Carreira, L. A.: Air-liquid partition coefficient for a diverse set of organic
932 compounds: Henry's law constant in water and hexadecane, *Environ. Sci. Technol.*, 42, 9231-9236, 2008.
933
934 Jensen, M. B.: On the kinetics of the decomposition of cyanic acid, *Acta Chem. Scand.*, 12, 1657-1670, 1958.
935
936 Jensen, M. B.: On the kinetics of the reaction of cyanic acid with amines, *Acta Chem. Scand.*, 13, 289-300, 1959.
937
938 Jimenez, J. L. and et al.: Evolution of organic aerosols in the atmosphere, *Science*, 326, 1525-1529, 2009.
939

940 Kames, J. and Schurath, U.: Henry's law and hydrolysis-rate constants for peroxyacetyl nitrates (PANs) using a
941 homogeneous gas-phase source, *J. Atmos. Chem.*, 21, 151-164, 1995.
942
943 Keller-Rudek, H., Moortgat, G. K., Sander, R., and Sorensen, R.: The MPI-Mainz UV/VIS spectral atlas of gaseous
944 molecules of atmospheric interest, *Earth Syst. Sci. Data*, 5, 365-373, 2013.
945
946 Kish, J. D., Leng, C., Kelley, J., Hiltner, J., Zhang, Y., and Liu, Y.: An improved approach for measuring Henry's
947 law coefficients of atmospheric organics, *Atmos Environ.*, 79, 561-565, 2013.
948
949 Kolb, C. E., Worsnop, D. R., Zahniser, M. S., Davidovits, P., Keyser, L. F., Leu, M.-T., Molina, M. J., Hanson, D.
950 R., Ravishankara, A. R., Williams, L. R., and Tolbert, M. A.: Laboratory studies of atmospheric heterogeneous
951 chemistry. In: *Progress and Problems in Atmospheric Chemistry*, Barker, J. R. (Ed.), *Advanced Series in Physical*
952 *Chemistry*, 3, World Scientific, Singapore, 1995.
953
954 Koss, A. R., K., S., Gilman, J. B., Selimovic, V., Coggon, M. M., Zarzana, K. J., Yuan, B., Lerner, B. M., Brown, S.
955 S., Jimenez, J. L., J., K., Roberts, J. M., Warneke, C., Yokelson, R. J., and de Gouw, J.: Non-methane organic gas
956 emissions from biomass burning: identification, quantification, and emission factors from PTR-ToF during the
957 FIREX 2016 laboratory experiment, *Atmos. Chem. Phys.*, 18, 3299-3319, 2018.
958
959 Kumar, V., Chandra, B. P., and Sinha, V.: Large unexplained suite of chemically reactive compounds present in
960 ambient air due to biomass fires., *Scientific Reports*, 8, 2018.
961
962 Lee, J. H., Na, C., Ramirez, R. L., and Olsen, T. M.: Cyanogen chloride precursor analysis in chlorinated river
963 water, *Environ. Sci. Technol.*, 40, 1478-1484, 2006.
964
965 Leo, A., Hansch, C., and Elkins, D.: Partition coefficients and their uses, *Chem. Rev.*, 71, 525-616, 1971.
966
967 Li, Q., Jacob, D. J., Bey, I., Yantosca, R. M., Zhao, Y., Kondo, Y., and Notholt, J.: Atmospheric hydrogen cyanide
968 (HCN): Biomass burning sources, ocean sink?, *Geophys. Res. Lett.*, 27, 357-360, 2000.
969
970 Lu, Z., Hebert, V. R., and Miller, G. C.: Gas-phase reaction of methyl isothiocyanate and methyl isocyanate with
971 hydroxyl radicals under static relative rate conditions, *J. Agric. Food Chem.*, 62, 1792-1795, 2014.
972
973 Maroulis, G. and Pouchan, C.: Dipole polarizability and hyperpolarizability of FCN, ClCN, BrCN and ICN, *Chem.*
974 *Phys.*, 216, 67-76, 1997.
975
976 Mattila, J. M., Brophy, P., Kirkland, J., Hall, S., Ullman, K., E.V., F., Brown, S., McDuffie, E., Tevlin, A., and
977 Farmer, D. K.: Tropospheric sources and sinks of gas-phase acids in the Colorado Front Range, *Atmos. Chem.*
978 *Phys.*, 18, 12315-12327, 2018.
979
980 McMaster, M. E., Ashley-Sing, C., Dos Santos Tavares, A. A., Corral, C. A., McGill, K., McNeil, D., Jansen, M. A.,
981 and Simpson, A. H. R. W.: The inhalation effects of by-products from chlorination of heated indoor swimming
982 pools on spinal development in pup mice, *Environ. Res.*, 166, 668-676, 2018.
983
984 Missner, A. and Pohl, P.: 110 Years of the Meyer–Overton rule: Predicting membrane permeability of gases and
985 other small compounds, *Chem Phys Chem*, 10, 1405-1414, 2009.
986
987 Na, C. and Olson, T. M.: Mechanism and kinetics of cyanogen chloride formation from the chlorination of glycine,
988 *Environ. Sci. Technol.*, 40, 1469-1477, 2006.
989
990 NASA: <https://espoarchive.nasa.gov/archive/browse/atom>, last access: Feb. 14 2019.
991
992 Raspoet, G., Nguyen, M. T., McGarraghy, M., and Hegarty, A. F.: The alcoholysis reaction of isocyanates giving
993 urethanes: Evidence for a multimolecular mechanism, *J. Org. Chem.*, 63, 6878-6885, 1998.
994

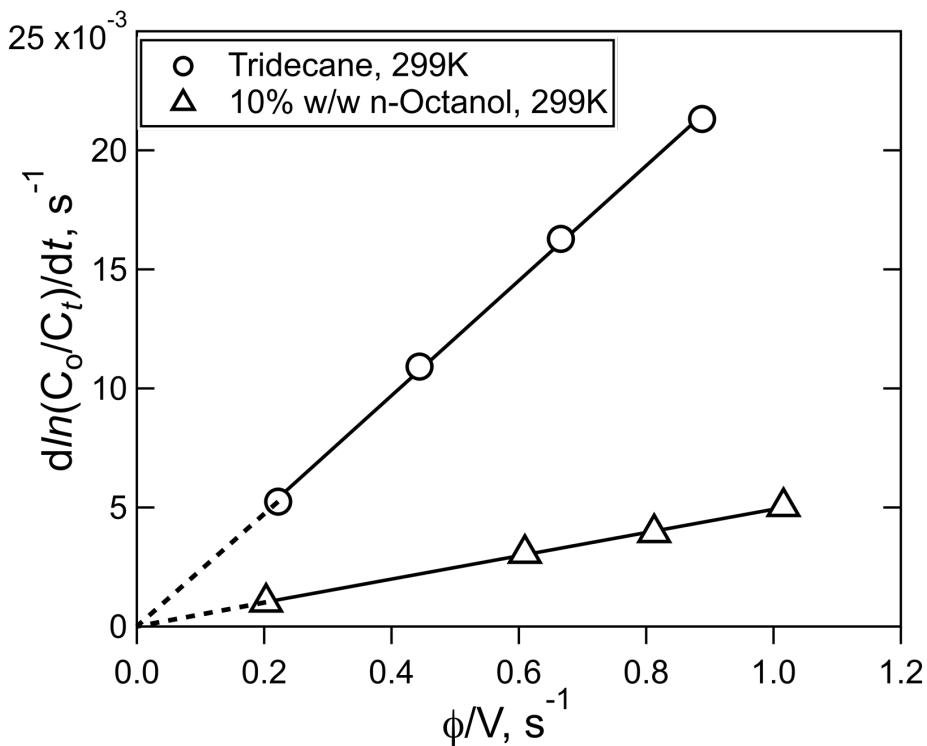
995 Reyes-Villegas, E., Bannan, T., Le Breton, M., Mehra, A., Priestley, M., Percival, C., Coe, H., and Allan, J. D.:
996 Online chemical characterization of food-cooking organic aerosols: Implications for Source Apportionment,
997 Environ. Sci. Technol., 52, 5308-5318, 2018.
998
999 Roberts, J. M.: Measurement of the Henry's law coefficient and the first order loss rate of PAN in n-octanol,
1000 Geophys. Res. Lett., 31, L08803, 2005.
1001
1002 Roberts, J. M., Osthoff, H. D., Brown, S. S., and Ravishankara, A. R.: N₂O₅ oxidizes chloride to Cl₂ in acidic
1003 atmospheric aerosol, Science, 321, 1059., 2008.
1004
1005 Roberts, J. M., Veres, P., Warneke, C., Neuman, J. A., Washenfelder, R. A., Brown, S. S., Baasandorj, M.,
1006 Burkholder, J. B., Burling, I. R., Johnson, T. J., Yokelson, R. J., and de Gouw, J.: Measurement of HONO, HNCO,
1007 and other inorganic acids by negative-ion proton-transfer chemical-ionization mass spectrometry (NI-PT-CIMS):
1008 Application to biomass burning emissions., Atmos. Meas. Tech., 3, 981-990, 2010.
1009
1010 Roberts, J. M., Veres, P. R., Cochran, A. K., Warneke, C., Burling, I. R., Yokelson, R. J., Lerner, B. M., Gilman, J.
1011 B., Kuster, W. C., Fall, R., and de Gouw, J.: Isocyanic acid in the atmosphere and its possible link to smoke-related
1012 health effects, PNAS, 108, 8966-8971, 2011.
1013
1014 Roberts, J. M., Veres, P. R., VandenBoer, T. C., Warneke, C., Graus, M., Williams, E. J., Holloway, J. S., Lefer, B.,
1015 Brock, C. A., Bahreini, R., Ozturk, F., Middlebrook, A. M., Wagner, N. L., Dube, W. P., and de Gouw, J. A.: New
1016 insights into atmospheric sources and sinks of isocyanic acid, HNCO, from recent urban and regional observations,
1017 J. Geophys. Res., 119, 2014.
1018
1019 Russell, J. A., McLaren, I. A., Jackson, W. M., and Halpern, J. B.: Photolysis of BrCN between 193 and 266 nm, J.
1020 Phys. Chem., 91, 3248-3253, 1987.
1021
1022 Sander, R.: Compilation of Henry's law constants (version 4.0) for water as solvent, Atmos. Chem. Phys., 15, 4399-
1023 4981, 2015.
1024
1025 Sander, R.: Modeling atmospheric chemistry: Interactions between gas-phase species and liquid cloud/aerosol
1026 particles, Surv. Geophys., 20, 1-31, 1999.
1027
1028 Sarkar, C., Sinha, V., Kumar, V., Rupakheti, M., Panday, A., Mahata, K. S., Rupakeheti, D., Kathayat, B., and
1029 Lawrence, M. G.: Overview of VOC emissions and chemistry from PTR-TOF-MS measurements during the
1030 SusKat-ABC campaign: high acetaldehyde, isoprene and isocyanic acid in wintertime air of the Kathmandu Valley,
1031 Atmos. Chem. Phys., 16, 3979-4003, 2016.
1032
1033 Saylor, R. D., Edgerton, E. S., Hartsell, B. E., Baumann, K., and Hansen, D. A.: Continuous gaseous and total
1034 ammonia measurements from the southeastern aerosol research and characterization (SEARCH) study, Atmos.
1035 Environ., 44, 4994-5004, 2010.
1036
1037 Schlorke, D., Flemming, J., Birkemeyer, C., and Arnhold, J.: Formation of cyanogen iodide by lactoperoxidase., J.
1038 Inorg. Biochem., 154, 35-41, 2016.
1039
1040 Schofield, D., Tsang, W., and Bauer, S. H.: Thermal decomposition of ClCN, J. Chem. Phys., 42, 2132 - 2137,
1041 1965.
1042
1043 Schreiber, J. and Witkop, B.: The reaction of cyanogen bromide with mono- and diamino Acids, J. Am. Chem. Soc.,
1044 86, 2441-2445, 1964.
1045
1046 Schumpe, A.: The estimation of gas solubilities in salt solutions, Chem. Eng. Sci., 48, 153-158, 1993.
1047
1048 Schwab, J. J., Li, Y., Bae, M.-S., Demerjian, K. L., Hou, J., Zhou, X., Jensen, B., and Pryor, S.: A laboratory
1049 intercomparison of real-time gaseous ammonia measurement methods, Environ. Sci. Technol., 41, 8412-8419,
1050 2007.

1051
1052 Shang, C., Gong, W.-l., and Blatchley III, E. R.: Breakpoint chemistry and volatile byproduct formation resulting
1053 from chlorination of model organic-N compounds, *Environ. Sci. Technol.*, 34, 1721-1728, 2000.
1054
1055 Siddiqui, S. and Siddiqui, B. S.: Some extensions of von Braun (BrCN) reaction on organic bases, *Z. Naturforsch.*,
1056 35b, 1049-1052, 1980.
1057
1058 Simpson, W. R., von Glasow, R., Riedel, K., Anderson, P., Ariya, P., Burrows, J., Carpenter, L. J., FrieB, U.,
1059 Goodsite, M. E., Heard, D., Hutterli, M., Jacobi, H.-W., Kaleschke, L., Neff, B., Plane, J., Platt, U., Richter, A.,
1060 Roscoe, H., Sander, R., Shepson, P., Sodeau, J., Steffen, A., Wagner, T., and Wolff, E.: Halogens and their role in
1061 polar boundary-layer ozone depletion, *Atmospheric Chemistry And Physics*, 7, 4375-4418, 2007.
1062
1063 State of California, OEHHA Chemical Database - Air: <https://oehha.ca.gov/air/chemicals/methyl-isocyanate>,
1064 accessed August 23, 2017.
1065
1066 Stockwell, C. E., Kupc, A., Witkowski, B., Talukdar, R. K., Liu, Y., Selimovic, V., Zarzana, K. J., Sekimoto, K.,
1067 Warneke, C., Washenfelder, R. A., Yokelson, R. J., Middlebrook, A. M., and Roberts, J. M.: Characterization of a
1068 catalyst-based conversion technique to measure total particle nitrogen and organic carbon and comparison to a
1069 particle mass measurement instrument, *Atmos. Meas. Tech.*, 11, 2749-2768, 2018.
1070
1071 Valentour, J. C., Aggarwal, V., and Sunshine, I.: Sensitive gas chromatographic determination of cyanide, *Anal.*
1072 *Chem.*, 46, 924-925, 1974.
1073
1074 Vanelslander, B., Paul, C., Grueneberg, J., Prince, E. K., Gillard, J., Sabbe, K., Pohnert, G., and Vyeverman, W.:
1075 Daily bursts of biogenic cyanogen bromide (BrCN) control biofilm formation around a marine benthic diatom.,
1076 *Proc. Natl Acad. Sci.*, 109, 2412-2417, 2012.
1077
1078 von Braun, J. and Schwarz, R.: Die einwirkung von bromcyan auf tertiäre amine, *Chem. Ber.*, 35, 1279-1285, 1902.
1079
1080 Wang, C., Lei, Y. D., Endo, S., and Wania, F.: Measuring and modeling the salting-out effect in ammonium sulfate
1081 solutions, *Environ. Sci. Technol.*, 48, 13238-13245, 2014.
1082
1083 Wang, Z., Nicholls, S. J., Rodriguez, E. R., Kumm, O., Hörkko, S., Barnard, J., Reynolds, W. F., Topol, E. J.,
1084 DiDonato, J. A., and Hazen, S. L.: Protein carbamylation links inflammation, smoking, uremia, and atherogenesis,
1085 *Nature Medicine*, 13, 1176-1184, 2007.
1086
1087 Weng, S.-C., Weaver, W. A., Blatchley, T. N., Cramer, J. S., Chen, J., and Blatchley III, E. R.: Dynamics of gas-
1088 phase trichloramine (NCl₃) in chlorinated, indoor swimming pool facilities, *Indoor Air*, 21, 391-399, 2011.
1089
1090 Wentzell, J. B., Liggio, J., Li, S.-M., Vlasenko, A., Staebler, R., Lu, G., Poitras, M.-J., Chan, T., and Brook, J. R.:
1091 Measurements of gas phase acids in Diesel exhaust: A relevant source of HNCO?, *Environ. Sci. Technol.*, 47, 7663-
1092 7671, 2013.
1093
1094 Wesely, M. L. and Hicks, B. B.: A review of the current status of knowledge on dry deposition, *Atmospheric*
1095 *Environment*, 34, 2261-2282, 2000.
1096
1097 Widner, B., Mulholland, M. R., and Mopper, K.: Chromatographic determination of nanomolar cyanate
1098 concentrations in estuarine and sea waters by precolumn fluorescence derivatization. , *Anal. Chem.*, 85, 6661-6666,
1099 2013.
1100
1101 Williams, A. and Jencks, W. P.: Acid and base catalysis of urea synthesis: Nonlinear Bronsted plots consistent with
1102 a diffusion-controlled proton-transfer mechanism and reactions of imidazole and N-methylimidazole with cyanic
1103 acids, *J. Chem. Soc., Perkins II*, 1974a. 1760-17868, 1974a.
1104
1105 Williams, A. and Jencks, W. P.: Urea Synthesis from amines and cyanic acid: kinetic evidence for a zwitterionic
1106 intermediate, *J. Chem. Soc., Perkins II*, , 1974b. 1753-1759, 1974b.

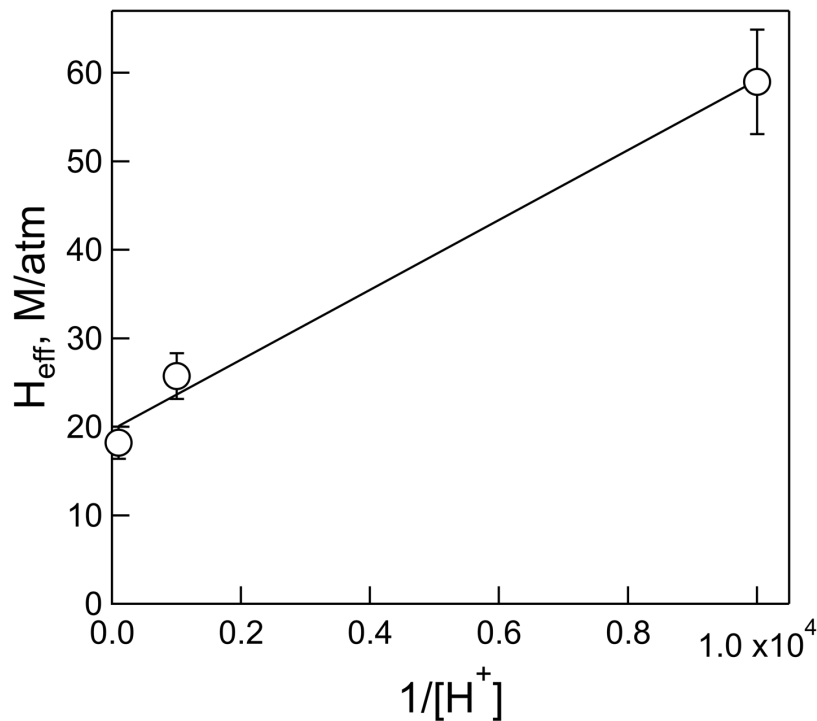
1107
1108 Williams, E. J., Baumann, K., Roberts, J. M., Bertman, S. B., Norton, R. B., Fehsenfeld, F. C., Springston, S. R.,
1109 Nunnermacker, L. J., Newman, L., Olszyna, K., Meagher, J., Hartsell, B., Edgerton, E., Pearson, J. R., and Rodgers,
1110 M. O.: Intercomparison of ground-based NO_y measurement techniques, *J. Geophys. Res.-Atmospheres*, 103, 22261-
1111 22280, doi: 22210.21029/22298JD00074, 1998.
1112
1113 Williams, J., Roberts, J. M., Bertman, S. B., Stroud, C. A., Fehsenfeld, F. C., Baumann, K., Buhr, M. P., Knapp, K.,
1114 Murphy, P. C., Nowick, M., and Williams, E. J.: A method for the airborne measurement of PAN, PPN, and MPAN,
1115 *J. Geophys. Res.-Atmos.*, 105, 28,943-928,960, 2000.
1116
1117 Woo, S.-C. and Liu, T.-K.: The absorption spectra and dissociation energies of cyanic acid and some isocyanates, *J.*
1118 *Chem. Phys.*, 3, 544-546, 1935.
1119
1120 Woodrow, J. E., LePage, J. T., Miller, G. C., and Herbert, V. R.: Determination of methyl isocyanate in outdoor
1121 residential air near metam-sodium soil fumigations, *J. Agric. Food Chem.*, 62, 8921-8927, 2014.
1122
1123 Woodward-Massey, R., Taha, Y. M., Moussa, S. G., and Osthoff, H. D.: Comparison of negative-ion proton-transfer
1124 with iodide ion chemical ionization mass spectrometry for quantification of isocyanic acid in ambient air, *Atmos*
1125 *Environ.*, 98, 693-703, 2014.
1126
1127 Yang, X. and Shang, C.: Chlorination byproduct formation in the presence of humic acid, model nitrogenous organic
1128 compounds, ammonia, and bromide, *Environ. Sci. Technol.*, 38, 4995-5001, 2004.
1129
1130 Yaws, C. L. and Yang, H.-C.: Henry's law constant for compounds in water. . In: *Thermodynamic and physical*
1131 *properties*, Yaws, C. L. (Ed.), Gulf Publishing Company, Houston, TX, 1992.
1132
1133 Young, P. J., Emmons, L. K., Roberts, J. M., Lamarque, J.-F., Wiedinmyer, C., Veres, P., and VandenBoer, T. C.:
1134 Isocyanic acid in a global chemistry transport model: Tropospheric distribution, budget, and identification of regions
1135 with potential health impacts, *J. Geophys. Res.-Atmos.*, 117, 2012.
1136
1137 Yuan, B., Koss, A. R., Warneke, C., Gilman, J. B., Lerner, B. M., Stark, H., and de Gouw, J. A.: A high-resolution
1138 time-of-flight chemical ionization mass spectrometer utilizing hydronium ions (H₃O⁺ ToF-CIMS) for measurements
1139 of volatile organic compounds in the atmosphere, *Atmos. Meas. Tech.*, 9, 2735-2752, 2016.
1140
1141 Zhao, R., Lee, A. K. Y., Wentzell, J. J. B., McDonald, A. M., Toom-Sauntry, D., Leaitch, W. R., Modini, R. L.,
1142 Corrigan, A. L., Russell, L. M., Noone, K. J., Schroder, J. C., Bertram, A. K., Hawkins, L. N., Abbatt, J. P. D., and
1143 Liggio, J.: Cloud partitioning of isocyanic acid (HNCO) and evidence of secondary source of HNCO in ambient air,
1144 *Geophys. Res. Lett.*, 41, 2014.
1145



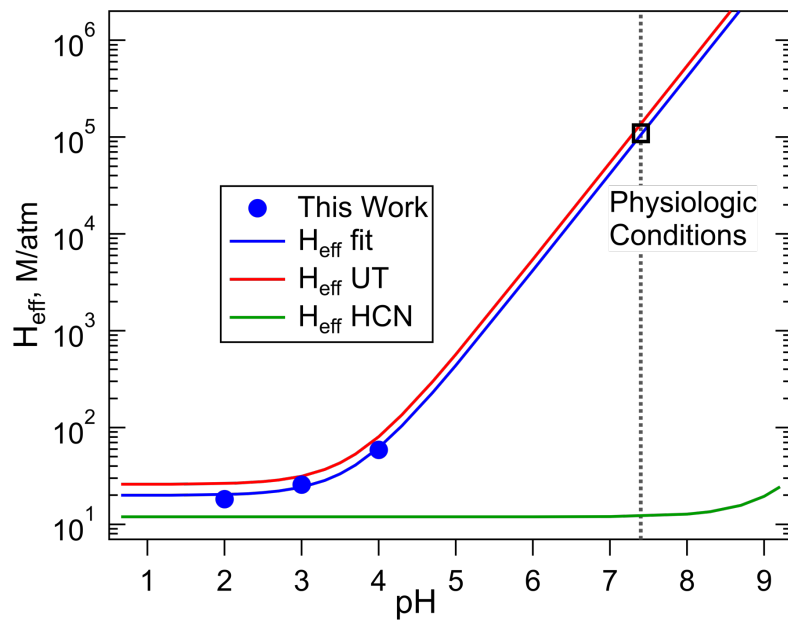
1147
1148 **Figure 1.** Plots of the ratio of HNCO concentration at time t , C_t , to the initial concentration, C_0 , versus time for a
1149 series of flow rates, noted as ambient cc/min. The solvent was tridecane ($C_{13}H_{28}$) and 299 K.
1150
1151



1152
1153 **Figure 2.** Plots of HNCO loss rate versus the ratio of volumetric flow rate, ϕ , to solution volume, V , for the
1154 experiment shown in Figure 1, (circles), and the experiment with 10% w/w n-octanol in tridecane at 299 K
1155 (triangles). The error bars in the individual rates were smaller than the width of the points.
1156

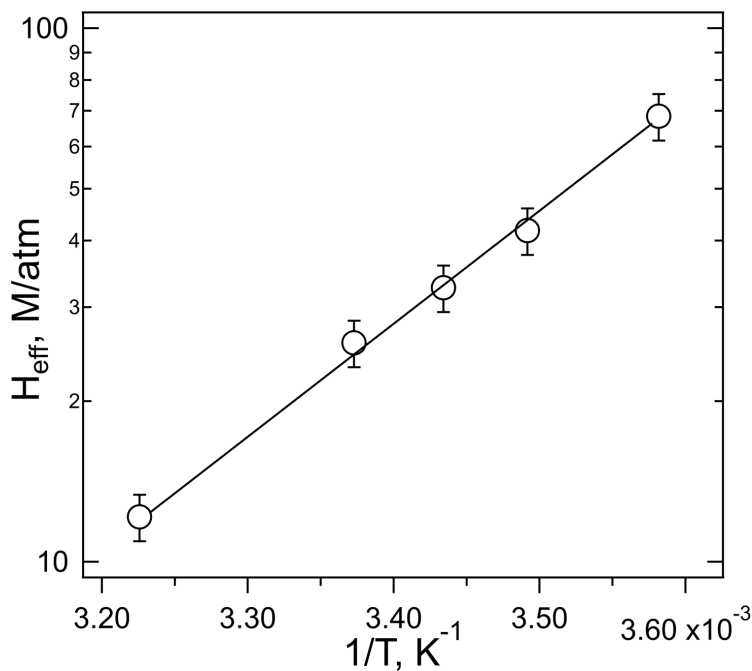


1157
 1158 Figure 3. Plot of effective Henry's coefficient of HNCO vs $1/[H^+]$ for the measurements at pH=2, pH=3 and pH=4,
 1159 and 298 K.
 1160
 1161



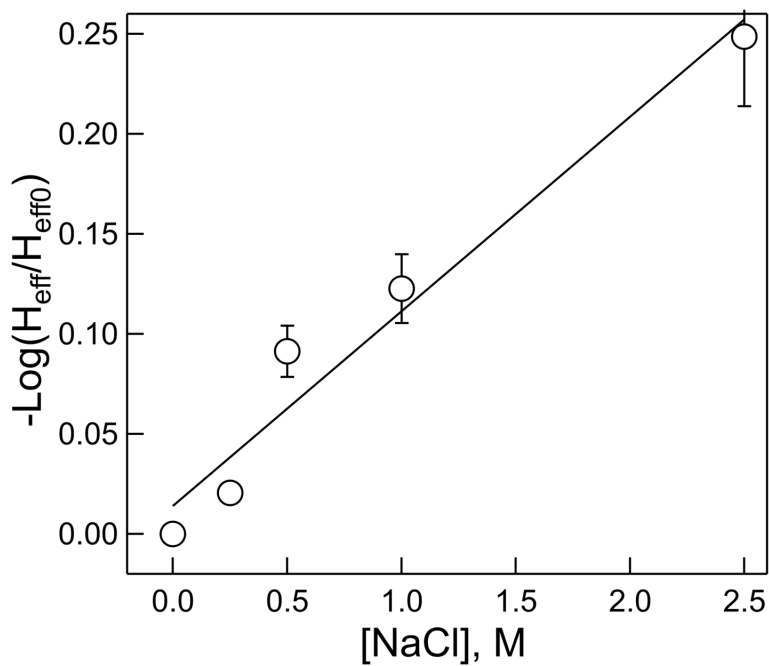
1162
 1163 Figure 4. Comparison of effective Henry's coefficients of HNCO measured in this work (blue) with those reported
 1164 by Borduas et al., 2016, plotted versus pH, according to Equation 4. The error bars on our H_{eff} values are smaller
 1165 than the width of the symbols. The green line was calculated for HCN from the intrinsic H coefficient reported by
 1166 Sander, (2015), and its pKa, 9.3.
 1167

1168



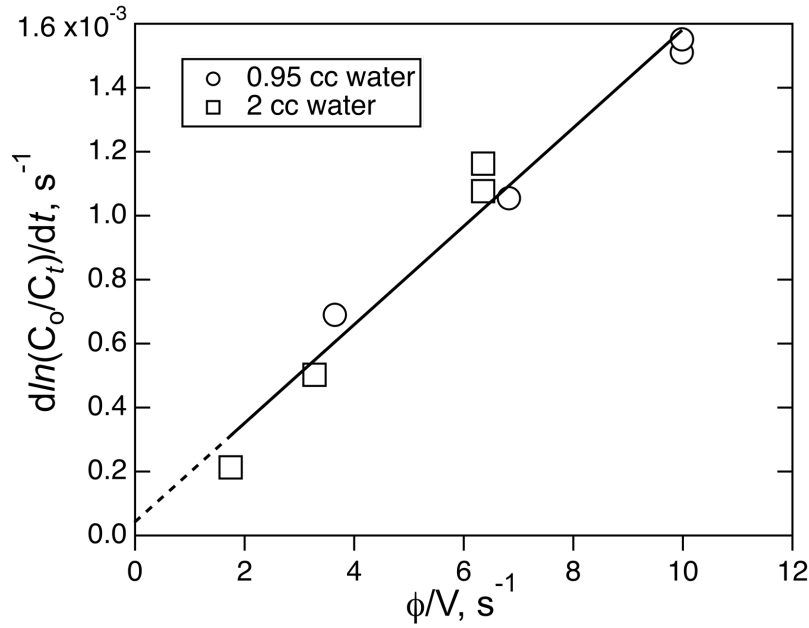
1169
1170
1171
1172
1173

Figure 5. The plot of $\ln H_{eff}$ vs $1/T$ for the experiments performed with HNCO at pH=3. $R^2=0.997$



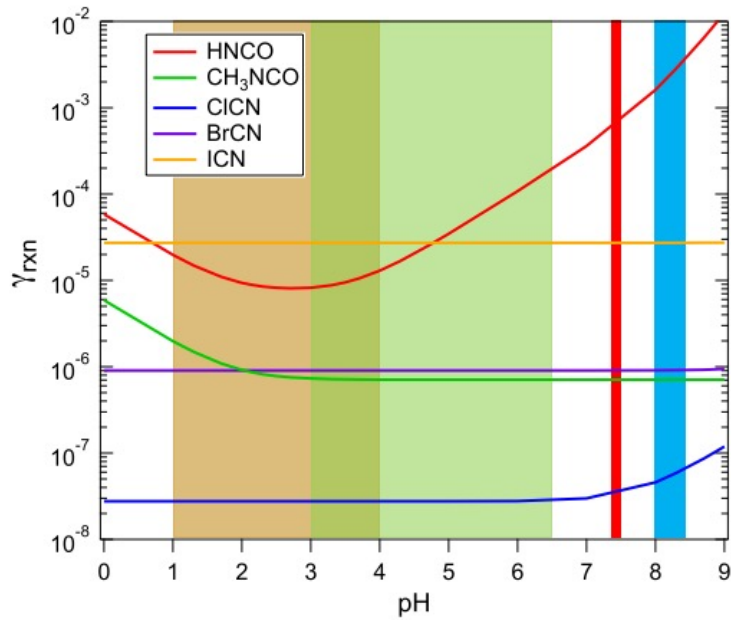
1174
1175
1176
1177
1178

Figure 6. Dependence of the effective Henry's coefficient (H) at a given salt concentration, relative to that with no added salt (H_{eff0}) versus NaCl molarity. $R^2 = 0.960$



1179
1180
1181
1182

Figure 7., The Plot of ICN loss rate versus the ratio of volumetric flow rate, ϕ , to solution volume, V , for the experiment involving the solubility of ICN in water with the small reactor. The line is the least-square fit to the data ($R^2 = 0.968$)



1183
1184
1185
1186

Figure 8. The uptake coefficients of HNCO, CH₃NCO, ClCN, BrCN, and ICN as a function of pH for aqueous solution at approximately 298 K. The shaded areas show the range of pHs characteristic of: aerosols (light brown), cloud/fog water (green), human physiology (red), and ocean surface water (light blue).

Table 1. Summary of solubility and loss rate measurements of HNCO and CH₃NCO.

Solute	Solvent	Temp. (°K)	pH	Salt, Reactant	H _{eff} , M/atm	Literature H	k ^l , (x10 ³), s ⁻¹	Literature k, (x10 ³), s ⁻¹
HNCO	H ₂ O	279	3.0		68 ±7	73 ^a	0.22	0.24 ^a 0.17 ^b
		286.5	3.0		42 ±4	51 ^a	0.38	0.43 ^a 0.41 ^b
		291	3.0		33 ±3	40 ^a	0.66	0.63 ^a 0.72 ^b
		296.5	3.0		26 ±2.6	31 ^a	1.02	0.96 ^a 1.32 ^b
		310	3.0		12 ±1.2	17 ^a	4.15	2.6 ^a 5.6 ^b
		298	2.0		18 ±1.8		2.2 ±0.1	
		298	3.0		26 ±2.6		1.02 ±0.13	
		298	4.0		59 ±5.9		0.72 ±0.11	
		298	3.0	0M NaCl	26 ±2.6			
		298	3.0	0.25M NaCl	24.6 ±2.5			
		298	3.0	0.5M NaCl	20.9 ±2.1			
		298	3.0	1.0M NaCl	19.4 ±2.0			
		298	3.0	2.5M NaCl	14.5 ±1.5			
		292	3.0	0.45M NH ₄ Cl	31.5 ±3.2		1.2	0.005 - 0.015 ^c
CH ₃ NCO	Tridecane (TD)	298	-		1.7 ±0.17		<0.043	
		283	-		13.2 ±1.6		0.16 ±0.18	
		298	-		8.3 ±0.8		<0.03	
		298	-	n-Octanol	87 ±9		<0.015	
		310	-	n-Octanol	51 ±5		0.057 ±0.014	
CH ₃ NCO	H ₂ O	298	2.0		1.3 ±0.13		3.2 ±0.3	2.5 ^d , 3.1 ^e
		298	7.0		1.4 ±0.14		1.9 ±0.6	1.34 ^d , 1.47 ^e
		298	-	n-Octanol	4.0 ±0.5		2.5 ±0.5	
		310	-	n-Octanol	2.8 ±0.3		5.3 ±0.7	

a. Calculated from the temperature and pH dependent data reported by Borduas et al., (2016).

b. Calculated from the temperature and pH dependent data reported by Jensen, (1958).

c. These were calculated from rates measured at higher pHs, assuming the mechanism is HNCO + NH₃ => H₂NC(O)NH₂

d. From k_{H+} and k_w reported by Williams and Jencks (1974a)

e. From k_{H+} for HCl and k_w reported by Castro et al., (1985)

Table 2. Summary of solubility and loss rate measurements of XCN compounds.

Solute	Solvent	Temp. (°K)	pH	H _{eff} , M/atm	Literature H	k ^l , (x10 ³), s ⁻¹	Literature k, (x10 ³), s ⁻¹
CICN	H ₂ O	299.5	7.0	1.4 ±0.14	0.6 ^a , 0.52 ^b	0.0 ±0.42	3.03 x10 ^{-3c}
	H ₂ O	273.15	7.0	4.5 ±0.4		0.015 ±0.016	
	n-Octanol	299.5		1.9 ±0.2		1.3 ±0.4	
BrCN	H ₂ O	296	7.0	8.2 ±0.8		6.2 ±3.7 x10 ⁻²	1.9 – 9.2 x10 ^{-2d}
	H ₂ O	273.15	7.0	32.7 ±3		2.4 ±0.5 x10 ⁻²	
	n-Octanol	297		31 ±3		9 ±2 x10 ⁻²	
ICN	H ₂ O	296	7.0	270 ±54		4.4 ±7.6 x10 ⁻²	~3.4 x10 ^{-2e}

a. Measured value at 293K, reported by Weng et al., (2011).

b. Modelled value at 298K, reported by Hilal et al., (2008).

c. From k_w and k_{OH} reported by Bailey and Bishop (1973).

d. Estimated from Heller-Grossman et al., 1999, and Vanelslander, et al., 2012.

e. Estimated from Gerritsen et al., (1993).

Table 3. Estimates of HNCO, CH₃NCO, and XCN compounds against loss due to heterogeneous processes.

Process	HNCO	CH₃NCO	ClCN	BrCN	ICN
BL deposition	1-2 days	0.5 yrs	yrs	0.5 yrs	5-10 days
Aerosol dep.	6-12 days	2-4 months	yrs	0.6 yrs	8 days
In-cloud rxn	2-6 hrs ^a	2 months	10-20 wks	1-3 wks	1-3 days

a. from the highly polluted case described by Barth et al., (2013).

Table 4. Octanol/Water partition coefficients for HNCO, CH₃NCO, ClCN, BrCN and related compounds.

Compound	Temperature	LogK _{ow}
HNCO ^a	298	0.64
	310	0.63
CH ₃ NCO	298	0.49
ClCN	299.5	0.13
BrCN	297	0.61 ^b
HC(O)OH	298	-0.54 ^c
CH ₃ NO ₂	293	-0.33 ^c
HCN	?	0.66 ^d
CH ₃ CN	298	-0.34 ^c

a. This uses the intrinsic H calculated from Eq(5), and our results.

b. based on extrapolated H_{H₂O} at 297K

c. (Sangster, 1989)

d. (EPA, 1989)